

12

Introduction to Switched-Capacitor Circuits

Our study of amplifiers in previous chapters has dealt with only cases where the input signal is continuously available and applied to the circuit and the output signal is continuously observed. Called “continuous-time” circuits, such amplifiers find wide application in audio, video, and high-speed analog systems. In many situations, however, we may sense the input only at periodic instants of time, ignoring its value at other times. The circuit then processes each “sample,” producing a valid output at the end of each period. Such circuits are called “discrete-time” or “sampled-data” systems.

In this chapter, we study a common class of discrete-time systems called “switched-capacitor (SC) circuits.” Our objective is to provide the foundation for more advanced topics such as filters, comparators, ADCs, and DACs. Most of our study deals with switched-capacitor amplifiers but the concepts can be applied to other discrete-time circuits as well. Beginning with a general view of SC circuits, we describe sampling switches and their speed and precision issues. Next, we analyze switched-capacitor amplifiers, considering unity-gain, noninverting, and multiply-by-two topologies. Finally, we examine a switched-capacitor integrator.

12.1 General Considerations

In order to understand the motivation for sampled-data circuits, let us first consider the simple continuous-time amplifier shown in Fig. 12.1(a). Used extensively with bipolar op amps, this circuit presents a difficult issue if implemented in CMOS technology. Recall that, to achieve a high voltage gain, the open-loop output resistance of CMOS op amps is maximized, typically approaching hundreds of kilo-ohms. We therefore suspect that R_2 heavily drops the open-loop gain, degrading the precision of the circuit. In fact, with the aid of the simple equivalent circuit

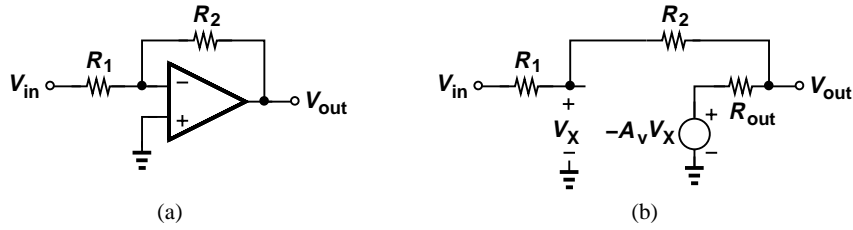


Figure 12.1. (a) Continuous-time feedback amplifier, (b) equivalent circuit of (a).

shown in Fig. 12.1(b), we can write

$$-A_v \left(\frac{V_{out} - V_{in}}{R_1 + R_2} R_1 + V_{in} \right) - R_{out} \frac{V_{out} - V_{in}}{R_1 + R_2} = V_{out}, \quad (12.1)$$

and hence

$$\frac{V_{out}}{V_{in}} = -\frac{R_2}{R_1} \cdot \frac{\frac{A_v - R_{out}}{R_2}}{1 + \frac{R_{out}}{R_1} + A_v + \frac{R_2}{R_1}}. \quad (12.2)$$

Equation (12.2) implies that, compared to the case where $R_{out} = 0$, the closed-loop gain suffers from inaccuracies in both the numerator and the denominator. Also, the input resistance of the amplifier, approximately equal to R_1 , loads the preceding stage while introducing thermal noise.

In the circuit of Fig. 12.1(a), the closed-loop gain is set by the ratio of R_2 and R_1 . In order to avoid reducing the open-loop gain of the op amp, we postulate that the resistors can be replaced by capacitors [Fig. 12.2(a)]. But, how is the bias voltage at node X set? We may add a large feedback

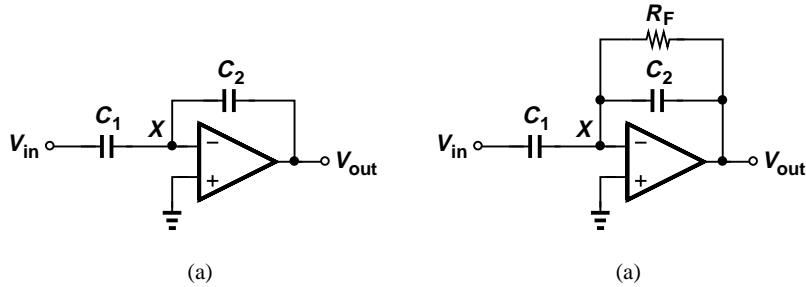


Figure 12.2. (a) Continuous-time feedback amplifier using capacitors, (b) use of resistor to define bias point.

resistor as in Fig. 12.2(b), providing dc feedback while negligibly affecting the ac behavior of the amplifier in the frequency band of interest. Such an arrangement is indeed practical if the circuit senses *only* high-frequency signals. But suppose, for example, the circuit is to amplify a voltage

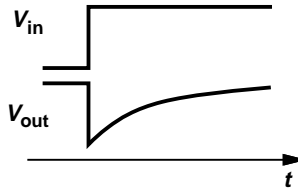


Figure 12.3. Step response of the amplifier of Fig. 12.2(b).

step. Illustrated in Fig. 12.3, the response contains a step change due to the initial amplification by the circuit consisting of C_1, C_2 , and the op amp, followed by a “tail” resulting from the loss of charge on C_2 through R_F . From another point of view, the circuit may not be suited to amplify *wideband* signals because it exhibits a high-pass transfer function. In fact, the transfer function is given by

$$\frac{V_{out}}{V_{in}}(s) \approx -\frac{\frac{R_F}{C_2 s}}{R_F + \frac{1}{C_2 s}} \div \frac{1}{C_1 s} \quad (12.3)$$

$$= -\frac{R_F C_1 s}{R_F C_2 s + 1}, \quad (12.4)$$

indicating that $V_{out}/V_{in} \approx -C_1/C_2$ only if $\omega \gg (R_F C_2)^{-1}$.

The above difficulty can be remedied by increasing $R_F C_2$, but in many applications the required values of the two components become prohibitively large. We must therefore seek other methods of establishing the bias while utilizing capacitive feedback networks.

Let us now consider the switched-capacitor circuit depicted in Fig. 12.4, where three switches control the operation: S_1 and S_3 connect the left plate of C_1 to V_{in} and ground, respectively, and

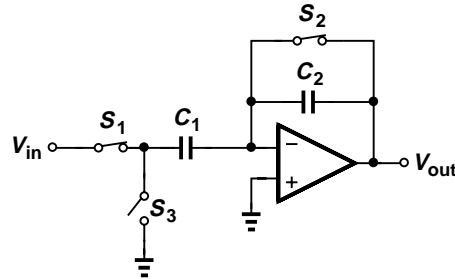


Figure 12.4. Switched-capacitor amplifier.

S_2 provides unity-gain feedback. We first assume the open-loop gain of the op amp is very large and study the circuit in two phases. First, S_1 and S_2 are on and S_3 is off, yielding the equivalent

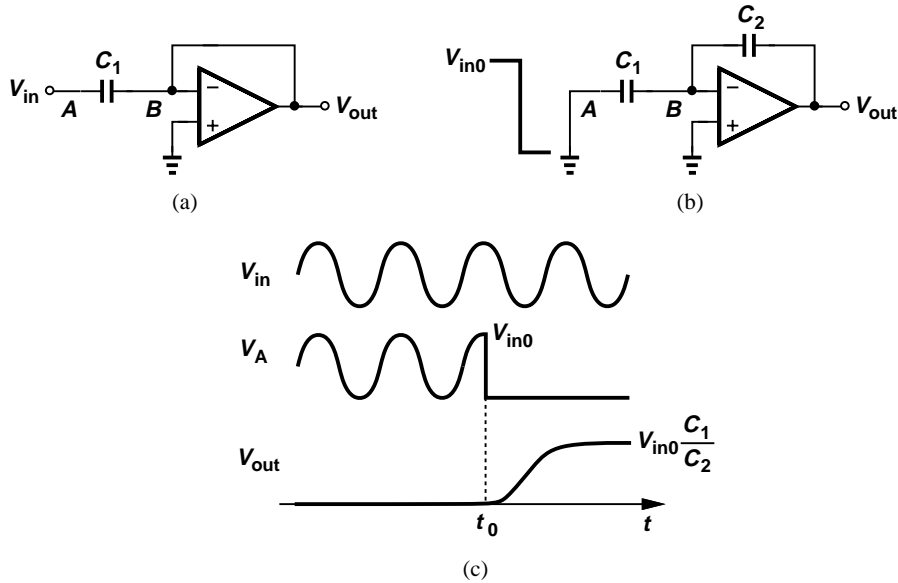


Figure 12.5. Circuit of Fig. 12.4 in (a) sampling mode, (b) amplification mode.

circuit of Fig. 12.5(a). For a high-gain op amp, $V_B = V_{out} \approx 0$, and hence the voltage across C_1 is approximately equal to V_{in} . Next, at $t = t_0$, S_1 and S_2 turn off and S_3 turns on, pulling node A to ground. Since V_A changes from V_{in0} to 0, the output voltage must change from zero to $V_{in0}C_1/C_2$.

The output voltage change can also be calculated by examining the transfer of charge. Note that the charge stored on C_1 just before t_0 is equal to $V_{in0}C_1$. After $t = t_0$, the negative feedback through C_2 drives the op amp input differential voltage and hence the voltage across C_1 to zero (Fig. 12.6). The charge stored on C_1 at $t = t_0$ must then be transferred to C_2 , producing an output

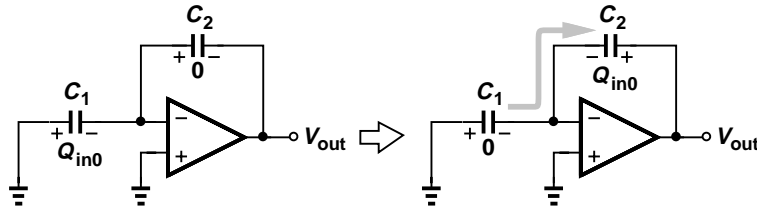


Figure 12.6. Transfer of charge from C_1 to C_2 .

voltage equal to $V_{in0}C_1/C_2$. Thus, the circuit amplifies V_{in0} by a factor of C_1/C_2 .

Several attributes of the circuit of Fig. 12.4 distinguish it from continuous-time implementations. First, the circuit devotes some time to “sample” the input, setting the output to zero and providing no amplification during this period. Second, after sampling, for $t > t_0$, the circuit ignores the input voltage V_{in} , amplifying the sampled voltage. Third, the circuit configuration changes

considerably from one phase to another, as seen in Fig. 12.5(a) and (b), raising concern about its stability.

What is the advantage of the amplifier of Fig. 12.4 over that in Fig. 12.1? In addition to sampling capability, we note from the waveforms depicted in Fig. 12.5 that after V_{out} settles, the current through C_2 approaches zero. That is, the feedback capacitor does not reduce the open-loop gain of the amplifier if the output voltage is given enough time to settle. In Fig. 12.1, on the other hand, R_2 continuously loads the amplifier.

The switched-capacitor amplifier of Fig. 12.4 lends itself to implementation in CMOS technology much more easily than in other technologies. This is because discrete-time operations require switches to perform sampling as well as a high input impedance to sense the stored quantities with no corruption. For example, if the op amp of Fig. 12.4 incorporates bipolar transistors at its input, the base current drawn from the inverting input in the amplification phase [Fig. 12.5(b)] creates an error in the output voltage. The existence of simple switches and a high input impedance have made CMOS technology the dominant choice for sampled-data applications.

The foregoing discussion leads to the conceptual view illustrated in Fig. 12.7 for switched-capacitor amplifiers. In the simplest case, the operation takes place in two phases: sampling and

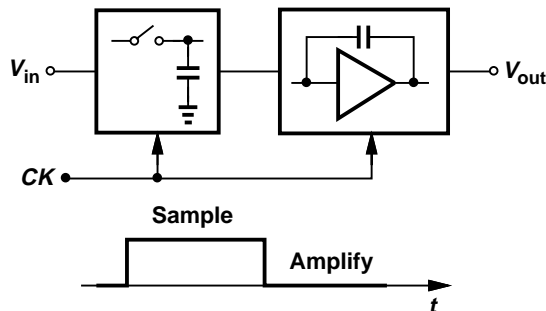


Figure 12.7. General view of switched-capacitor amplifier.

amplification. Thus, in addition to the analog input, V_{in} , the circuit requires a clock to define each phase.

Our study of SC amplifiers proceeds according to these two phases. First, we analyze various sampling techniques. Second, we consider SC amplifier topologies.

12.2 Sampling Switches

12.2.1 MOSFETS as Switches

A simple sampling circuit consists of a switch and a capacitor [Fig. 12.8(a)]. A MOS transistor can serve as a switch [Fig. 12.8(b)] because (a) it can be on while carrying zero current, and (b) its

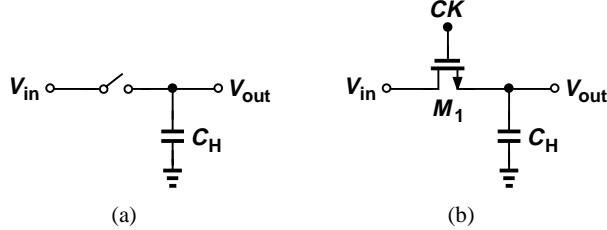


Figure 12.8. (a) Simple sampling circuit, (b) implementation of the switch by a MOS device.

source and drain voltages are not “pinned” to the gate voltage, i.e., if the gate voltage varies, the source or drain voltage need not follow that variation. By contrast, bipolar transistors lack both of these properties, typically necessitating complex circuits to perform sampling.

To understand how the circuit of Fig. 12.8(b) samples the input, first consider the simple cases depicted in Fig. 12.9, where the gate command, CK , goes high at $t = t_0$. In Fig.

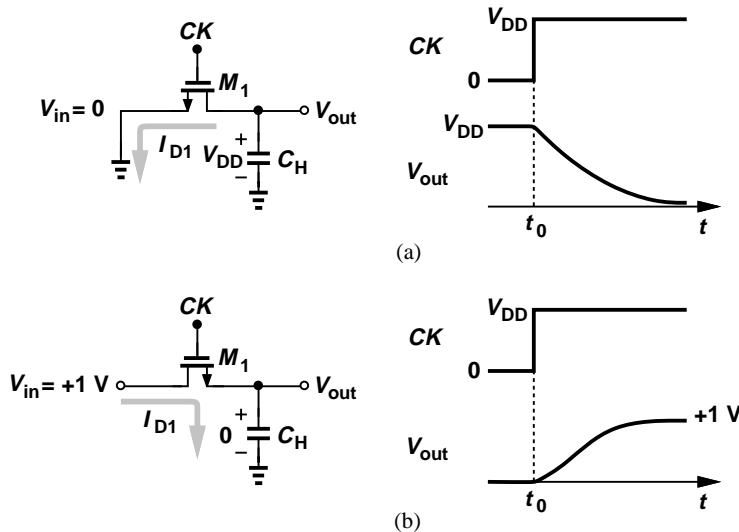


Figure 12.9. Response of a sampling circuit to different input levels and initial conditions.

12.9(a), we assume that $V_{in} = 0$ for $t \geq t_0$ and the capacitor has an initial voltage equal to V_{DD} . Thus, at $t = t_0$, M_1 senses a gate-source voltage equal to V_{DD} while its drain voltage is also equal to V_{DD} . The transistor therefore operates in saturation, drawing a current of $I_{D1} =$

$(\mu_n C_{ox}/2)(W/L)(V_{DD} - V_{TH})^2$ from the capacitor. As V_{out} falls, at some point $V_{out} = V_{DD} - V_{TH}$, driving M_1 into the triode region. The device nevertheless continues to discharge C_H until V_{out} approaches zero. We note that for $V_{out} \ll 2(V_{DD} - V_{TH})$, the transistor can be viewed as a resistor equal to $R_{on} = [\mu_n C_{ox}(W/L)(V_{DD} - V_{TH})]^{-1}$.

Now consider the case in Fig. 12.9(b), where $V_{in} = +1$ V, $V_{out}(t = t_0) = 0$ V, and $V_{DD} = 3$ V. Here, the terminal of M_1 connected to C_H acts as the source, and the transistor turns on with $V_{GS} = +3$ V, but $V_{DS} = +1$ V. Thus, M_1 operates in the triode region, charging C_H until V_{out} approaches +1 V. For $V_{out} \approx +1$ V, M_1 exhibits an on-resistance of $R_{on} = [\mu_n C_{ox}(W/L)(V_{DD} - V_{in} - V_{TH})]^{-1}$.

The above observations reveal two important points. First, a MOS switch can conduct current in either direction simply by exchanging the role of its source and drain terminals. Second, as shown in Fig. 12.10, when the switch is on, V_{out} follows V_{in} and when the switch is off, V_{out} remains

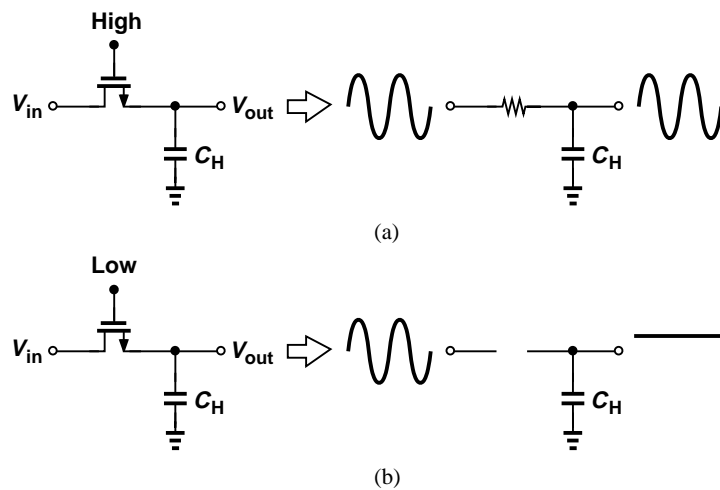


Figure 12.10. Track and hold capabilities of a sampling circuit.

constant. Thus, the circuit “tracks” the signal when CK is high and “freezes” the instantaneous value of V_{in} across C_H when CK goes low.

Example 12.1

In the circuit of Fig. 12.9(a), calculate V_{out} as a function of time. Assume $\lambda = 0$.

Solution. Before V_{out} drops below $V_{DD} - V_{TH}$, M_1 is saturated and we have:

$$V_{out}(t) = V_{DD} - \frac{I_{D1}t}{C_H} \quad (12.5)$$

$$= V_{DD} - \frac{1}{2}\mu_n C_{ox} \frac{W}{L} (V_{DD} - V_{TH})^2 \frac{t}{C_H}. \quad (12.6)$$

After

$$t_1 = \frac{2V_{TH}C_H}{\mu_n C_{ox} \frac{W}{L} (V_{DD} - V_{TH})^2}, \quad (12.7)$$

M_1 enters the triode region, yielding a time-dependent current. We therefore write:

$$C_H \frac{dV_{out}}{dt} = -I_{D1} \quad (12.8)$$

$$= -\frac{1}{2}\mu_n C_{ox} \frac{W}{L} [2(V_{DD} - V_{TH})V_{out} - V_{out}^2] \quad t > t_1. \quad (12.9)$$

Rearranging (12.9), we have

$$\frac{dV_{out}}{[2(V_{DD} - V_{TH}) - V_{out}]V_{out}} = -\frac{1}{2}\mu_n \frac{C_{ox}}{C_H} \frac{W}{L} dt, \quad (12.10)$$

which, upon separation into partial fractions, is written as

$$\left[\frac{1}{V_{out}} + \frac{1}{2(V_{DD} - V_{TH}) - V_{out}} \right] \frac{dV_{out}}{V_{DD} - V_{TH}} = -\mu_n \frac{C_{ox}}{C_H} \frac{W}{L} dt. \quad (12.11)$$

Thus,

$$\ln V_{out} - \ln[2(V_{DD} - V_{TH}) - V_{out}] = -(V_{DD} - V_{TH})\mu_n \frac{C_{ox}}{C_H} \frac{W}{L} (t - t_1), \quad (12.12)$$

that is,

$$\ln \frac{V_{out}}{2(V_{DD} - V_{TH}) - V_{out}} = -(V_{DD} - V_{TH})\mu_n \frac{C_{ox}}{C_H} \frac{W}{L} (t - t_1). \quad (12.13)$$

Taking the exponential of both sides and solving for V_{out} , we obtain

$$V_{out} = \frac{2(V_{DD} - V_{TH}) \exp[-(V_{DD} - V_{TH})\mu_n \frac{C_{ox}}{C_H} \cdot \frac{W}{L} (t - t_1)]}{1 + \exp[-(V_{DD} - V_{TH})\mu_n \frac{C_{ox}}{C_H} \cdot \frac{W}{L} (t - t_1)]}. \quad (12.14)$$

In the circuit of Fig. 12.9(b), we assumed $V_{in} = +1$ V (Fig. 12.11). Now suppose $V_{in} = V_{DD}$.

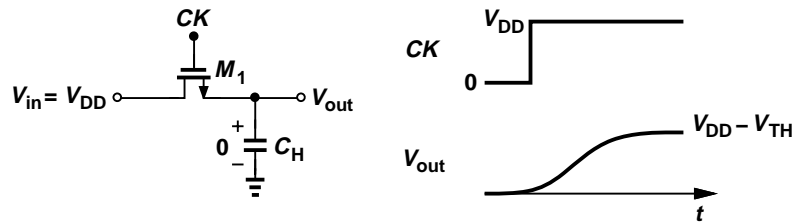


Figure 12.11. Maximum output level in an NMOS sampler.

How does V_{out} vary with time? Since the gate and drain of M_1 are at the same potential, the transistor is **saturated** and we have:

$$C_H \frac{dV_{out}}{dt} = I_{D1} \quad (12.15)$$

$$= \frac{1}{2} \mu_n C_{ox} \frac{W}{L} (V_{DD} - V_{out} - V_{TH})^2, \quad (12.16)$$

where channel-length modulation is neglected. It follows that

$$\frac{dV_{out}}{(V_{DD} - V_{out} - V_{TH})^2} = \frac{1}{2} \mu_n \frac{C_{ox}}{C_H} \frac{W}{L} dt, \quad (12.17)$$

and hence

$$\frac{1}{V_{DD} - V_{out} - V_{TH}} \Big|_0^{V_{out}} = \frac{1}{2} \mu_n \frac{C_{ox}}{C_H} \frac{W}{L} t \Big|_0^t, \quad (12.18)$$

where body effect is neglected and $V_{out}(t = 0)$ is assumed zero. Thus,

$$V_{out} = V_{DD} - V_{TH} - \frac{1}{\frac{1}{2} \mu_n \frac{C_{ox}}{C_H} \frac{W}{L} t + \frac{1}{V_{DD} - V_{TH}}}. \quad (12.19)$$

Equation (12.19) implies that as $t \rightarrow \infty$, $V_{out} \rightarrow V_{DD} - V_{TH}$. This is because as V_{out} approaches $V_{DD} - V_{TH}$, the **overdrive voltage of M_1 vanishes**, reducing the current available for charging C_H to negligible values. Of course, even for $V_{out} = V_{DD} - V_{TH}$, the **transistor conducts some subthreshold current** and, given enough time, eventually brings V_{out} to V_{DD} . Nonetheless, as mentioned in Chapter 3, for typical operation speeds, it is reasonable to assume that V_{out} does not exceed $V_{DD} - V_{TH}$.

The foregoing analysis demonstrates a serious limitation of MOS switches: if the **input signal level is close to V_{DD}** , then the output provided by an NMOS switch cannot track the input. From another point of view, the **on-resistance of the switch increases considerably** as the input and output voltages approach $V_{DD} - V_{TH}$. We may then ask: what is the maximum input level that the switch can pass to the output faithfully? In Fig. 12.11, for $V_{out} \approx V_{in}$, the transistor must operate in deep triode region and hence the **upper bound of V_{in} equals $V_{DD} - V_{TH}$** . As explained below, in practice V_{in} must be quite lower than this value.

Example 12.2

In the circuit of Fig. 12.12, calculate the minimum and maximum on-resistance of M_1 . Assume $\mu_n C_{ox} = 50 \mu\text{A/V}^2$, $W/L = 10/1$, $V_{TH} = 0.7 \text{ V}$, $V_{DD} = 3 \text{ V}$, and $\gamma = 0$.

Solution. We note that in the steady state, M_1 remains in the triode region because the gate voltage is higher than both V_{in} and V_{out} by a value greater than V_{TH} . If $f_{in} = 10 \text{ MHz}$, we predict

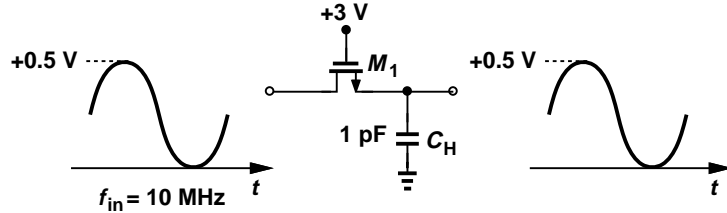


Figure 12.12.

that V_{out} tracks V_{in} with a negligible phase shift due to the on-resistance of M_1 and C_H . Assuming $V_{out} \approx V_{in}$, we need not distinguish between the source and drain terminals, obtaining

$$R_{on1} = \frac{1}{\mu_n C_{ox} \frac{W}{L} (V_{DD} - V_{in} - V_{TH})}. \quad (12.20)$$

Thus, $R_{on1,max} \approx 1.11 \text{ k}\Omega$ and $R_{on1,min} \approx 870 \Omega$. By contrast, if the maximum input level is raised to 1.5 V, then $R_{on1,max} = 2.5 \text{ k}\Omega$.

MOS devices operating in **deep triode region** are sometimes called “zero-offset” switches to emphasize that they exhibit no dc shift between the input and output voltages of the simple sampling circuit of Fig. 12.8(b).¹ This is evident from examples of Fig. 12.9, where the output eventually becomes equal to the input. Nonexistent in bipolar technology, the zero offset property proves crucial in precise sampling of analog signals.

We have thus far considered only NMOS switches. The reader can verify that the foregoing principles apply to PMOS switches as well. In particular, as shown in Fig. 12.13, a PMOS transistor fails to operate as a zero-offset switch if its gate is grounded and its drain terminal senses an input

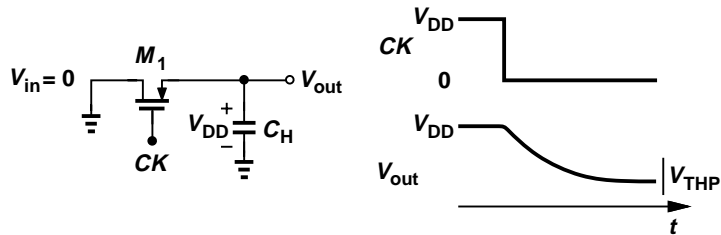


Figure 12.13. Sampling circuit using PMOS switch.

voltage of $|V_{THP}|$ or less. In other words, the on-resistance of the device rises rapidly as the input and output levels drop to $|V_{THP}|$ above ground.

¹We assume the circuit following the sampler draws no input dc current.

12.2.2 Speed Considerations

What determines the speed of the sampling circuits of Fig. 12.8? We must first define the speed here. Illustrated in Fig. 12.14, a simple, but versatile measure of speed is the time required for

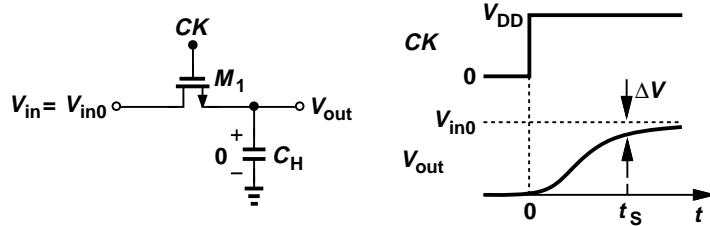


Figure 12.14. Definition of speed in a sampling circuit.

the output voltage to go from zero to the maximum input level after the switch turns on. Since V_{out} would take infinite time to become equal to V_{in0} , we consider the output settled when it is within a certain “error band,” ΔV , around the final value. For example, we say the output settles to 0.1% accuracy after t_S seconds, meaning that in Fig. 12.14, $\Delta V/V_{in0} = 0.1\%$. Thus, the speed specification must be accompanied by an accuracy specification as well. Note that after $t = t_S$, we can consider the source and drain voltages to be approximately equal.

From the circuit of Fig. 12.14, we surmise that the sampling speed is given by two factors: the on-resistance of the switch and the value of the sampling capacitor. Thus, to achieve a higher speed, a large aspect ratio and a small capacitor must be used. However, as illustrated in Fig. 12.12, the on-resistance also depends on the input level, yielding a greater time constant for more positive inputs (in the case of NMOS switches). From Eq. (12.20), we plot the on-resistance of the switch as a function of the input level [Fig. 12.15(a)], noting the sharp rise as V_{in} approaches

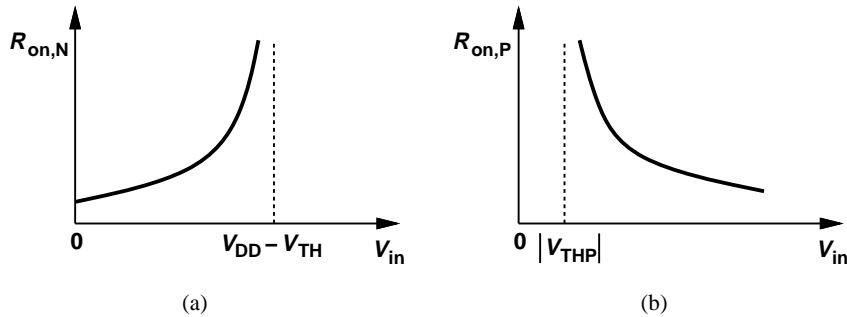


Figure 12.15. On-resistance of (a) NMOS and (b) PMOS devices as a function of input voltage.

$V_{DD} - |V_{TH}|$. For example, if we restrict the variation of R_{on} to a range of 4 to 1, then the maximum

input level is given by

$$\frac{1}{\mu_n C_{ox} \frac{W}{L} (V_{DD} - V_{in,max} - V_{TH})} = \frac{4}{\mu_n C_{ox} \frac{W}{L} (V_{DD} - V_{TH})}. \quad (12.21)$$

That is,

$$V_{in,max} = \frac{3}{4}(V_{DD} - V_{TH}). \quad (12.22)$$

This value falls around $V_{DD}/2$, translating to severe swing limitations. Note that the device threshold voltage directly limits the voltage swings.²

In order to accommodate greater voltage swings in a sampling circuit, we first observe that a PMOS switch exhibits an on-resistance that *decreases* as the input voltage becomes more positive [Fig. 12.15(b)]. It is then plausible to employ “complementary” switches so as to allow rail-to-tail swings. Shown in Fig. 12.16(a), such a combination requires complementary clocks, producing

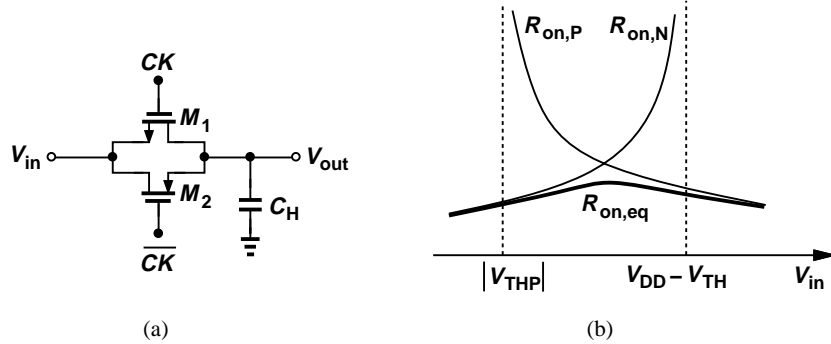


Figure 12.16. (a) Complementary switch, (b) on-resistance of the complementary switch.

an equivalent resistance:

$$R_{on,eq} = R_{on,N} \parallel R_{on,P} \quad (12.23)$$

$$= \frac{1}{\mu_n C_{ox} (\frac{W}{L})_N (V_{DD} - V_{in} - V_{THN})} \parallel \frac{1}{\mu_n C_{ox} (\frac{W}{L})_P (V_{in} - |V_{THP}|)} \quad (12.24)$$

$$= \frac{1}{\mu_n C_{ox} (\frac{W}{L})_N (V_{DD} - V_{THN}) - [\mu_n C_{ox} (\frac{W}{L})_N - \mu_p C_{ox} (\frac{W}{L})_P] V_{in} - \mu_p C_{ox} (\frac{W}{L})_P V_{THP}} \quad (12.25)$$

Interestingly, if $\mu_n C_{ox} (W/L)_N = \mu_p C_{ox} (W/L)_P$, then $R_{on,eq}$ is independent of the input level.³ Fig. 12.16(b) plots the behavior of $R_{on,eq}$ in the general case, revealing much less variation than that corresponding to each switch alone.

²By contrast, the output swing of cascode stages is typically limited by overdrive voltages rather than the threshold voltage.

³In reality, V_{THN} and V_{THP} vary with V_{in} through body effect but we ignore this variation here.

For high-speed input signals, it is critical that the NMOS and PMOS switches in Fig. 12.16(a) turn off simultaneously so as to avoid ambiguity in the sampled value. If, for example, the NMOS device turns off Δt seconds earlier than the PMOS device, then the output voltage tends to track the input for the remaining Δt seconds, but with a large, input-dependent time constant (Fig. 12.17). This effect gives rise to distortion in the sampled value. For moderate precision, the simple circuit

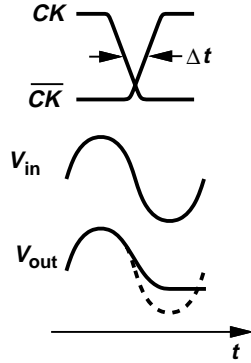


Figure 12.17. Distortion generated if complementary switches do not turn off simultaneously.

shown in Fig. 12.18 provides complementary clocks by duplicating the delay of inverter I_1 through

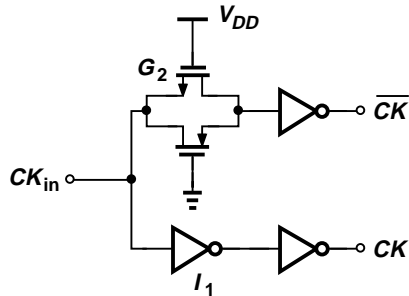


Figure 12.18. Simple circuit generating complementary clocks.

the gate G_2 .

12.2.3 Precision Considerations

Our foregoing study of MOS switches indicates that a larger W/L or a smaller sampling capacitor results in a higher speed. In this section, we show that these methods of increasing the speed degrade the precision with which the signal is sampled.

Three mechanisms in MOS transistor operation introduce error at the instant the switch turns off. We study each effect individually.

Channel Charge Injection Consider the sampling circuit of Fig. 12.19 and recall that for a MOSFET to be on, a channel must exist at the oxide-silicon interface. Assuming $V_{in} \approx V_{out}$, we

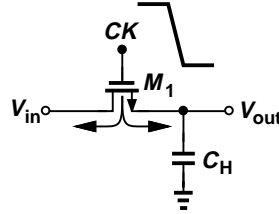


Figure 12.19. Charge injection when a switch turns off.

use our derivations in Chapter 2 to express the total charge in the inversion layer as

$$Q_{ch} = WLC_{ox}(V_{DD} - V_{in} - V_{TH}), \quad (12.26)$$

where L denotes the effective channel length. When the switch turns off, Q_{ch} exits through the source and drain terminals, a phenomenon called “channel charge injection.”

The charge injected to the left side on Fig. 12.19 is absorbed by the input source, creating no error. On the other hand, the charge injected to the right side is deposited on C_H , introducing an error in the voltage stored on the capacitor. For example, if half of Q_{ch} is injected onto C_H , the resulting error equals

$$\Delta V = \frac{WLC_{ox}(V_{DD} - V_{in} - V_{TH})}{2C_H}. \quad (12.27)$$

Illustrated in Fig. 12.20, the error for an NMOS switch appears as a negative “pedestal” at the

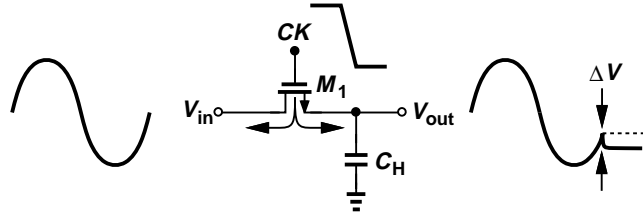


Figure 12.20. Effect of charge injection.

output. Note that the error is directly proportional to WLC_{ox} and inversely proportional to C_H .

An important question that arises now is: why did we assume in arriving at (12.27) that exactly *half* of the channel charge is injected onto C_H ? In reality, the fraction of charge that exits through the source and drain terminals is a relatively complex function of various parameters such as the impedance seen at each terminal to ground and the transition time of the clock [1, 2]. Investigations

of this effect have not yielded any rule of thumb that can predict the charge splitting in terms of such parameters. Furthermore, in many cases, these parameters, e.g., the clock transition time, are poorly controlled. Also, most circuit simulation programs model charge injection quite inaccurately. As a worst-case estimate, we can assume that the entire channel charge is injected onto the sampling capacitor.

How does charge injection affect the precision? Assuming all of the charge is deposited on the capacitor, we express the sampled output voltage as

$$V_{out} \approx V_{in} - \frac{WLC_{ox}(V_{DD} - V_{in} - V_{TH})}{C_H}, \quad (12.28)$$

where the phase shift between the input and output is neglected. Thus,

$$V_{out} = V_{in}\left(1 + \frac{WLC_{ox}}{C_H}\right) - \frac{WLC_{ox}}{C_H}(V_{DD} - V_{TH}), \quad (12.29)$$

suggesting that the output deviates from the ideal value through two effects: a non-unity gain equal to $1 + WLC_{ox}/C_H$,⁴ and a constant offset voltage $-WLC_{ox}(V_{DD} - V_{TH})/C_H$ (Fig. 12.21). In other words, since we have assumed channel charge is a *linear* function of the input voltage, the circuit exhibits only gain error and dc offset.

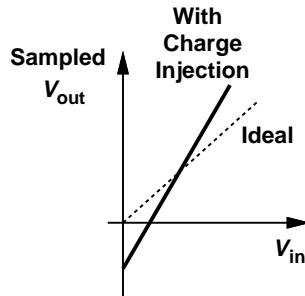


Figure 12.21. Input/output characteristic of sampling circuit in the presence of charge injection.

In the foregoing discussion, we tacitly assumed that V_{TH} is constant. However, for NMOS switches (in an n -well technology), body effect must be taken into account.⁵ Since $V_{TH} = V_{TH0} + \gamma(\sqrt{2\phi_B + V_{BS}} - \sqrt{2\phi_B})$, and $V_{BS} \approx -V_{in}$, we have

$$V_{out} = V_{in} - \frac{WLC_{ox}}{C_H}(V_{DD} - V_{in} - V_{TH0} - \gamma\sqrt{2\phi_B + V_{in}} - \gamma\sqrt{2\phi_B}), \quad (12.30)$$

$$= V_{in}\left(1 - \frac{WLC_{ox}}{C_H}\right) - \gamma\frac{WLC_{ox}}{C_H}\sqrt{2\phi_B + V_{in}} - \frac{WLC_{ox}}{C_H}(V_{DD} - V_{TH0} - \gamma\sqrt{2\phi_B}). \quad (12.31)$$

⁴The voltage gain is *greater* than unity because the pedestal becomes smaller as the input level rises.

⁵Even for PMOS switches, the n -well is connected to the most positive supply voltage because the source and drain terminals of the switch may interchange during sampling.

It follows that the nonlinear dependence of V_{TH} upon V_{in} introduces nonlinearity in the input/output characteristic.

In summary, charge injection contributes three types of errors in MOS sampling circuits: gain error, dc offsets, and nonlinearity. In many applications, the first two can be tolerated or corrected whereas the last cannot.

It is instructive to consider the speed-precision trade-off resulting from charge injection. Representing the speed by a simple time constant τ and the precision by the error ΔV due to charge injection, we define a figure of merit as $F = (\tau \Delta V)^{-1}$. Writing

$$\tau = R_{on} C_H \quad (12.32)$$

$$= \frac{1}{\mu_n C_{ox} (W/L) (V_{DD} - V_{in} - V_{TH})} C_H, \quad (12.33)$$

and

$$\Delta V = \frac{WLC_{ox}}{C_H} (V_{DD} - V_{in} - V_{TH}), \quad (12.34)$$

we have

$$F = \frac{\mu_n}{L^2}. \quad (12.35)$$

Thus, to the first order, the trade-off is independent of the switch width and the sampling capacitor.

Clock Feedthrough In addition to channel charge injection, a MOS switch couples the clock transitions to the sampling capacitor through its gate-drain or gate-source overlap capacitance. Depicted in Fig. 12.22, the effect introduces an error in the sampled output voltage. Assuming the

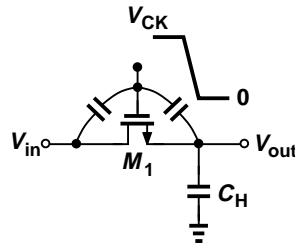


Figure 12.22. Clock feedthrough in a sampling circuit.

overlap capacitance is constant, we express the error as

$$\Delta V = V_{CK} \frac{WC_{ov}}{WC_{ov} + C_H}, \quad (12.36)$$

where C_{ov} is the overlap capacitance per unit width. The error ΔV is independent of the input level, manifesting itself as a constant offset in the input/output characteristic. As with charge injection, clock feedthrough leads to a trade-off between speed and precision as well.

kT/C Noise Recall from Example 7.1 that a resistor charging a capacitor gives rise to a total rms noise voltage of $\sqrt{kT/C}$. As shown in Fig. 12.23, a similar effect occurs in sampling circuits.

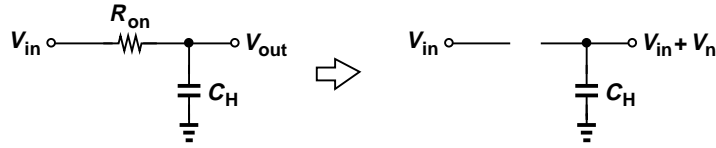


Figure 12.23. Thermal noise in a sampling circuit.

The **on-resistance of the switch** introduces thermal noise at the output and, when the switch turns off, this noise is stored on the capacitor along with the instantaneous value of the input voltage. It can be proved that the rms voltage of the sampled noise in this case is still approximately equal to $\sqrt{kT/C}$ [3, 4].

The problem of KT/C noise limits the performance in many high-precision applications. In order to achieve a low noise, the **sampling capacitor must be sufficiently large**, thus loading other circuits and degrading the speed.

12.2.4 Charge Injection Cancellation

The dependence of **charge injection** upon the input level and the trade-off expressed by (12.35) make it necessary to seek methods of cancelling the effect of charge injection so as to achieve a higher F . We consider a few such techniques here.

To arrive at the first technique, we postulate that the charge injected by the main transistor can be *removed* by means of a second transistor. As shown in Fig. 12.24, a “dummy” switch, M_2 , driven by \overline{CK} is added to the circuit such that after M_1 turns off and M_2 turns on, the channel

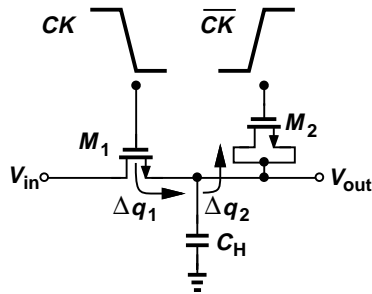


Figure 12.24. Addition of dummy device to reduce charge injection and clock feedthrough.

charge deposited by the former on C_H is **absorbed by the latter to create a channel**. Note that both the source and drain of M_2 are connected to the output node.

How do we ensure that the charge injected by M_1 , Δq_1 , is equal to that absorbed by M_2 , Δq_2 ? Suppose half of the channel charge of M_1 is injected onto C_H , i.e.,

$$\Delta q_1 = \frac{W_1 L_1 C_{ox}}{2} (V_{CK} - V_{in} - V_{TH1}). \quad (12.37)$$

Since $\Delta q_2 = W_2 L_2 C_{ox} (V_{CK} - V_{in} - V_{TH2})$, if we choose $W_2 = 0.5W_1$ and $L_2 = L_1$, then $\Delta q_2 = \Delta q_1$. Unfortunately, the assumption of equal splitting of charge between source and drain is generally invalid, making this approach less attractive.

Interestingly, with the choice $W_2 = 0.5W_1$ and $L_2 = L_1$, the effect of clock feedthrough is suppressed. As depicted in Fig. 12.25, the total charge in V_{out} is zero because

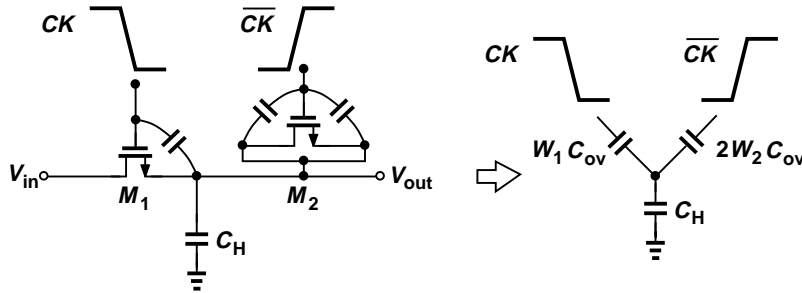


Figure 12.25. Clock feedthrough suppression by dummy switch.

$$-V_{CK} \frac{W_1 C_{ov}}{W_1 C_{ov} + C_H + 2W_2 C_{ov}} + V_{CK} \frac{2W_2 C_{ov}}{W_1 C_{ov} + C_H + 2W_2 C_{ov}} = 0. \quad (12.38)$$

Another approach to lowering the effect of charge injection incorporates both PMOS and NMOS devices such that the opposite charge packets injected by the two cancel each other (Fig. 12.26). For Δq_1 to cancel Δq_2 , we must have $W_1 L_1 C_{ox} (V_{CK} - V_{in} - V_{THN}) = W_2 L_2 C_{ox} (V_{in} - |V_{THP}|)$.

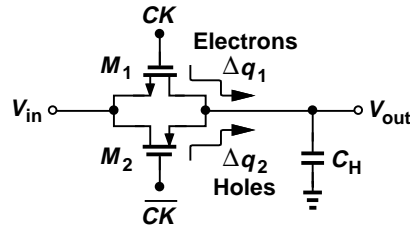


Figure 12.26. Use of complementary switches to reduce charge injection.

Thus, the cancellation occurs for only one input level. Even for clock feedthrough, the circuit does not provide complete cancellation because the gate-drain overlap capacitance of NFETs is not equal to that of PFETs.

Our knowledge of the advantages of differential circuits suggests that the problem of charge injection may be relieved through differential operation. As shown in Fig. 12.27, we surmise that the charge injection appears as a common-mode disturbance. But, writing $\Delta q_1 = WLC_{ox}(V_{CK} -$

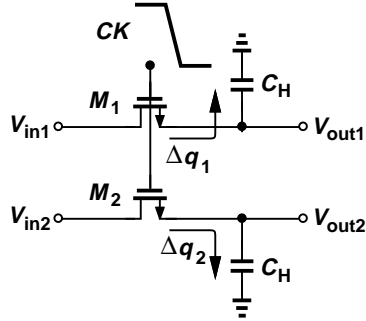


Figure 12.27. Differential sampling circuit.

$V_{in1} - V_{TH1}$), and $\Delta q_2 = WLC_{ox}(V_{CK} - V_{in2} - V_{TH2})$, we recognize that $\Delta q_1 = \Delta q_2$ only if $V_{in1} = V_{in2}$. In other words, the overall error is not suppressed for differential signals. Nevertheless, this technique both removes the constant offset and lowers the nonlinear component. This can be understood by writing

$$\Delta q_1 - \Delta q_2 = WLC_{ox}[(V_{in2} - V_{in1}) + (V_{TH2} - V_{TH1})] \quad (12.39)$$

$$= WLC_{ox}[V_{in2} - V_{in1} + \gamma(\sqrt{2\phi_F + V_{in2}} - \sqrt{2\phi_F + V_{in1}})]. \quad (12.40)$$

Since for $V_{in1} = V_{in2}$, $\Delta q_1 - \Delta q_2 = 0$, the characteristic exhibits no offset. Also, the nonlinearity of body effect now appears in both square-root terms of (12.40), leading to only odd-order distortion (Chapter ??).

The problem of charge injection continues to limit the speed-precision envelope in sampled-data systems. Many cancellation techniques have been introduced but each leading to other trade-offs. One such technique, called “bottom-plate sampling,” is widely used in switched-capacitor circuits and is described later in this chapter.

12.3 Switched-Capacitor Amplifiers

As mentioned in Section 12.1 and exemplified by the circuit of Fig. 12.4, CMOS feedback amplifiers are more easily implemented with a capacitive feedback network than a resistive one. Having examined sampling techniques, we are now ready to study a number of switched-capacitor amplifiers. Our objective is to understand the underlying principles as well as the speed-precision trade-offs encountered in the design of each circuit.

Before studying SC amplifiers, it is helpful to briefly look at the physical implementation of capacitors in CMOS technology. A simple capacitor structure is shown in Fig. 12.28(a), where the “top plate” is realized by a polysilicon layer and the “bottom plate” by a heavily-doped n^+ region.

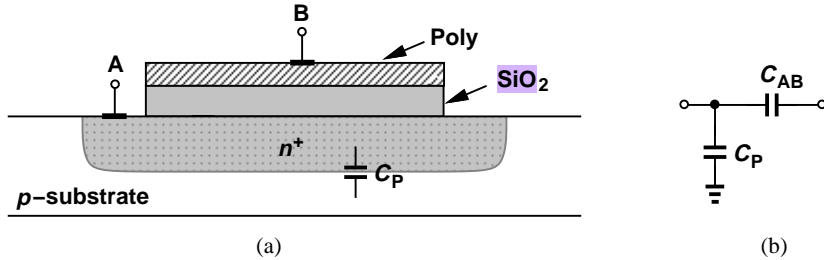


Figure 12.28. (a) Monolithic capacitor structure, (b) circuit model of (a) including parasitic capacitance to the substrate.

The dielectric is the thin oxide layer used in MOS devices as well.⁶ An important concern in using this structure is the parasitic capacitance between each plate and the substrate. In particular, the bottom plate suffers from substantial junction capacitance to the underlying p region - typically about 10 to 20% of the oxide capacitance. For this reason, we usually model the capacitor as in Fig. 12.28(b). Monolithic capacitors are described in more detail in Chapters ?? and ??.

12.3.1 Unity-Gain Sampler/Buffer

While a unity-gain amplifier can be realized with no resistors or capacitors in the feedback network [Fig. 12.29(a)], for discrete-time applications, it still requires a sampling circuit. We may therefore

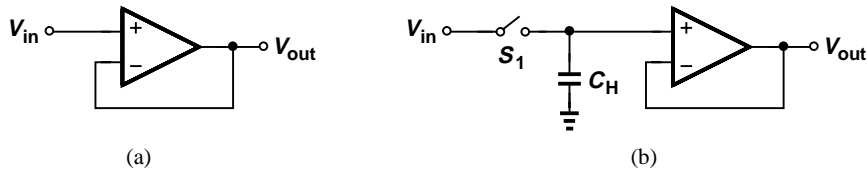


Figure 12.29. (a) Unity-gain buffer, (b) sampling circuit followed by unity-gain buffer.

conceive the circuit shown in Fig. 12.29(b) as a sampler/buffer. However, the input-dependent charge injected by S_1 onto C_H limits the accuracy here.

Now consider the topology depicted in Fig. 12.30(a), where three switches control the sampling and amplification modes. In the sampling mode, S_1 and S_2 are on and S_3 is off, yielding the topology

⁶The oxide thickness in this type of amplifier is typically thicker than that of MOS gate area because silicon dioxide grows faster on a heavily-doped material.

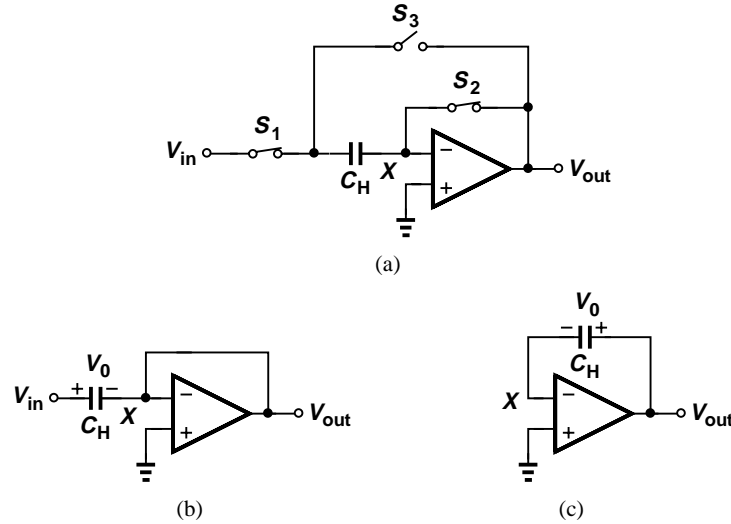


Figure 12.30. (a) Unity-gain sampler, (b) circuit of (a) in sampling mode, (c) circuit of (a) in amplification mode.

shown in Fig. 12.30(b). Thus, $V_{out} = V_X \approx 0$, and the voltage across C_H tracks V_{in} . At $t = t_0$, when $V_{in} = V_0$, S_1 and S_2 turn off and S_3 turns on, placing the capacitor around the op amp and entering the circuit into the amplification mode [Fig. 12.30(c)]. Since the op amp's high gain requires that node X still be a virtual ground and since the charge on the capacitor must be conserved, V_{out} rises to a value approximately equal to V_0 . This voltage is therefore “frozen” and it can be processed by subsequent stages.

With proper timing, the circuit of Fig. 12.30(a) can substantially alleviate the problem of channel charge injection. As Fig. 12.31 illustrates in “slow motion,” in the transition from the

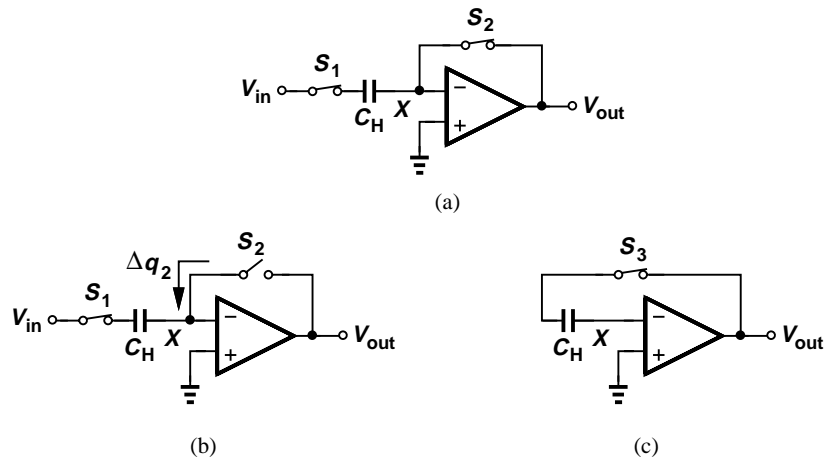


Figure 12.31. Operation of the unity-gain sampler in slow motion.

sampling mode to the amplification mode, S_2 turns off slightly *before* S_1 does. We carefully

examine the effect of the charge injected by S_2 and S_1 . When S_2 turns off, it injects a charge packet Δq_2 onto C_H , producing an error equal to $\Delta q_2/C_H$. However, this charge is quite independent of the input level because node X is a virtual ground. For example, if S_2 is realized by an NMOS device whose gate voltage equals V_{CK} , then $\Delta q_2 = WLC_{ox}(V_{CK} - V_{TH} - V_X)$. Although body effect makes V_{TH} a function of V_X , Δq_2 is relatively constant because V_X is quite independent of V_{in} .

The constant magnitude of Δq_2 means that channel charge of S_2 introduces only an offset (rather than gain error or nonlinearity) in the input/output characteristic. As described below, this offset can easily be removed by differential operation. But, how about the charge injected by S_1 onto C_H ? Let us set V_{in} to zero and suppose S_1 injects a charge packet Δq_1 onto node P [Fig. 12.32(a)]. If the capacitance connected from X to ground (including the input capacitance of the op amp) is

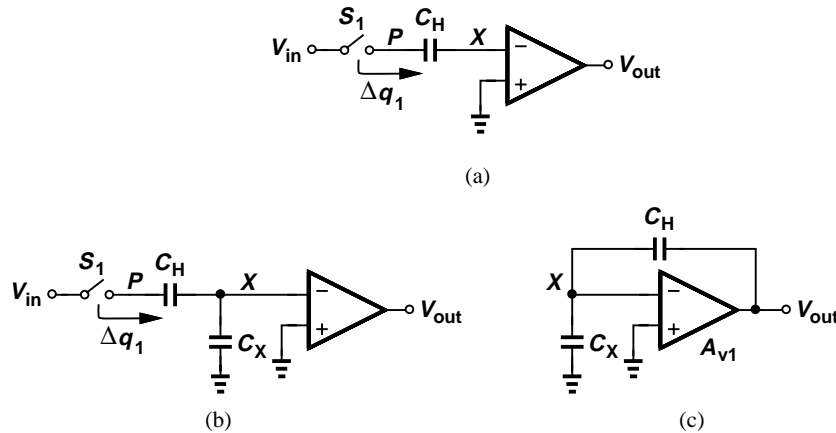


Figure 12.32. Effect of charge injected by S_1 with (a) zero and (b) finite op amp input capacitance, (c) transition of circuit to amplification mode.

zero, V_P and V_X jump to infinity. To simplify the analysis, we assume a total capacitance equal to C_X from X to ground [Fig. 12.32(b)], and we will see shortly that its value does not affect the results. In Fig. 12.32(b), each of C_H and C_X carries a charge equal to Δq_1 . Now, as shown in Fig. 12.32(c), we place C_H around the op amp, seeking to obtain the resulting output voltage.

To calculate the output voltage, we must make an important observation: the total charge at node X cannot change after S_2 turns off because no path exists for electrons to flow into or out of this node. Thus, if before S_1 turns off, the total charge on the right plate of C_H and the top plate of C_X is zero, it must still add up to zero after S_1 injects charge because no resistive path is connected to X . The same holds true after C_H is placed around the op amp.

Now consider the circuit of Fig. 12.32(c), assuming the the total charge at node X is zero. We can write $C_X V_X - (V_{out} - V_X)C_H = 0$, and $V_X = -V_{out}/A_{v1}$. Thus, $-(C_X + C_H)V_{out}/A_{v1} -$

$V_{out}C_H = 0$, i.e., $V_{out} = 0$. Note that this result is independent of Δq_1 , capacitor values, or the gain of the op amp, thereby revealing that the charge injection by S_1 introduces no error if S_2 turns off first.

In summary, in Fig. 12.30(a), after S_2 turns off, node X “floats,” maintaining a constant total charge regardless of the transitions at other nodes of the circuit. As a result, after the feedback configuration is formed, the output voltage is not influenced by the charge injection due to S_1 . From another point of view, node X is a virtual ground at the moment S_2 turns off, freezing the instantaneous input level across C_H and yielding a charge equal to $V_0 C_H$ on the left plate of C_H . After settling with feedback, node X is again a virtual ground, forcing C_H to still carry $V_0 C_H$ and hence the output voltage to be approximately equal to $V_0 C_H$.

The effect of the charge injected by S_1 can be studied from yet another perspective. Suppose in Fig. 12.32(c), the output voltage is finite and positive. Then, since $V_X = V_{out}/(-A_{v1})$, V_X must be finite and negative, requiring negative charge on the top plate of C_X . For the total charge at X to be zero, the charge on the left plate of C_H must be positive and that on its right plate negative, giving $V_{out} < 0$. Thus, the only valid solution is $V_{out} = 0$.

The third switch in Fig. 12.30(a), S_3 , also merits attention. In order to turn on, S_3 must establish an inversion layer at its oxide interface. Does the required channel charge come from C_H or from the op amp? We note from the foregoing analysis that after the feedback circuit has settled, the charge on C_H equals $V_0 C_H$, unaffected by S_3 . The channel charge of this switch is therefore entirely supplied by the op amp, introducing no error.

Our study of Fig. 12.30(a) thus far suggests that, with proper timing, the charge injected by S_1 and S_3 is unimportant and the channel charge of S_2 results in a constant offset voltage. Fig. 12.33 depicts a simple realization of the clock edges to ensure S_1 turns off after S_2 does.

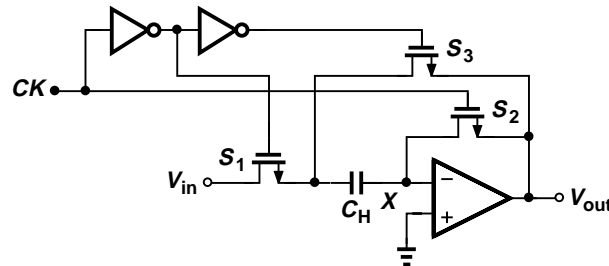


Figure 12.33. Generation of proper clock edges for unity-gain sampler.

The input-independent nature of the charge injected by the reset switch allows complete cancellation by differential operation. Illustrated in Fig. 12.34, such an approach employs a differential op amp along with two sampling capacitors so that the charge injected by S_2 and S'_2 appears as a

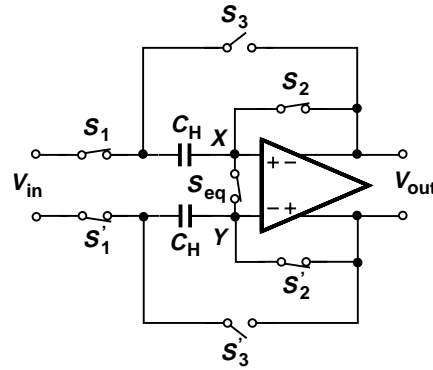


Figure 12.34. Differential realization of unity-gain sampler.

common-mode disturbance at nodes X and Y . This is in contrast to the behavior of the differential circuit shown in Fig. 12.27, where the input-dependent charge injection still leads to nonlinearity. In reality, S_2 and S'_2 exhibit a **finite charge injection mismatch**, an issue resolved by adding another switch, S_{eq} , that turns off slightly after S_2 and S'_2 (and before S_1 and S'_1), thereby equalizing the charge at nodes X and Y .

Precision Considerations The circuit of Fig. 12.30(a) operates as a **unity-gain buffer** in the amplification mode, producing an output voltage approximately equal to the voltage stored across the capacitor. How close to unity is the gain here? As a general case, we assume the op amp exhibits a finite input capacitance C_{in} and calculate the output voltage when the circuit goes from the sampling mode to the amplification mode (Fig. 12.35). Owing to the finite gain of the op amp, $V_X \neq 0$ in the amplification mode, giving a charge equal to $C_{in}V_X$ on C_{in} . The

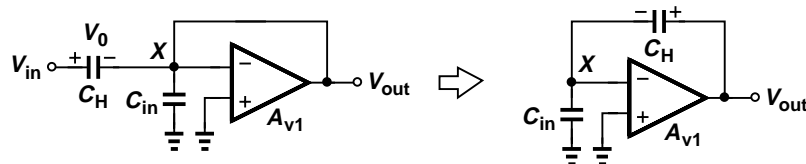


Figure 12.35. Equivalent circuit for accuracy calculations.

conservation of charge at X requires that $C_{in}V_X$ come from C_H , raising the charge on C_H to $C_H V_0 + C_{in}V_X$.⁷ It follows that the voltage across C_H equals $(C_H V_0 + C_{in}V_X)/C_H$. We therefore

⁷The charge on C_H increases because moving positive charge from the left plate of C_H to the top plate of C_{in} leads to a more positive voltage across C_H .

write $V_{out} = (C_H V_0 + C_{in} V_X)/C_H = V_X$ and $V_X = -V_{out}/A_{v1}$. Thus,

$$V_{out} = \frac{V_0}{1 + \frac{1}{A_{v1}} \left(\frac{C_{in}}{C_H} + 1 \right)} \quad (12.41)$$

$$\approx V_0 \left[1 - \frac{1}{A_{v1}} \left(\frac{C_{in}}{C_H} + 1 \right) \right]. \quad (12.42)$$

As expected, if $C_{in}/C_H \ll 1$, then $V_{out} \approx V_0/(1 + A_{v1}^{-1})$. In general, however, the circuit suffers from a gain error of approximately $-(C_{in}/C_H + 1)/A_{v1}$, suggesting that the input capacitance must be minimized even if speed is not critical. Recall from Chapter 9 that to increase A_{v1} , we may choose a large width for the input transistors of the op amp, but at the cost of higher input capacitance. An optimum device size must therefore yield minimum gain error rather than maximum A_{v1} .

Example 12.3

In the circuit of Fig. 12.35, $C_{in} = 0.5$ pF and $C_H = 2$ pF. What is the minimum op amp gain that guarantees a gain error of 0.1%?

Solution. Since $C_{in}/C_H = 0.25$, we have $A_{v1,min} = 1000 \times 1.25 = 1250$.

Speed Considerations Let us first examine the circuit in the sampling mode [Fig. 12.36(a)]. What is the time constant in this phase? The total resistance in series with C_H is given by R_{on1}

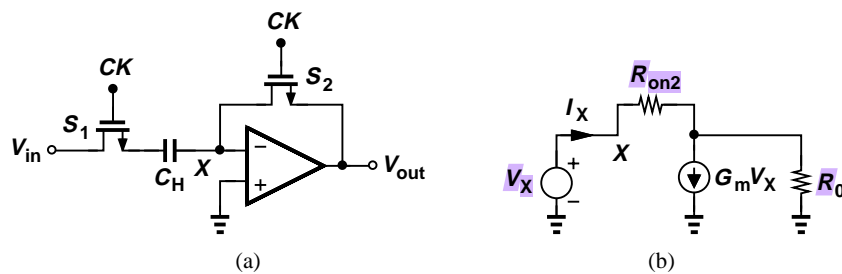


Figure 12.36. (a) Unity-gain sampler in sampling mode, (b) equivalent circuit of (a).

and the resistance between X and ground, R_X . Using the simple op amp model shown in Fig. 12.36(b), where R_0 denotes the open-loop output impedance of the op amp, we have

$$(I_X - G_m V_X)R_0 + I_X R_{on2} = V_X, \quad (12.43)$$

that is,

$$R_X = \frac{R_0 + R_{on2}}{1 + G_m R_0}. \quad (12.44)$$

Since typically $R_{on2} \ll R_0$ and $G_m R_0 \gg 1$, we have $R_X \approx 1/G_m$. For example, in a telescopic op amp employing differential to single-ended conversion, G_m equals the transconductance of each input transistor.

The time constant in the sampling mode is thus equal to

$$\tau_{sam} = (R_{on1} + \frac{1}{G_m})C_H. \quad (12.45)$$

The magnitude of τ_{sam} must be sufficiently small to allow settling in the test case of Fig. 12.14 to the required precision.

Now let us consider the circuit as it enters the amplification mode. Shown in Fig. 12.37 along with both the op amp input capacitance and the load capacitance, the circuit must begin

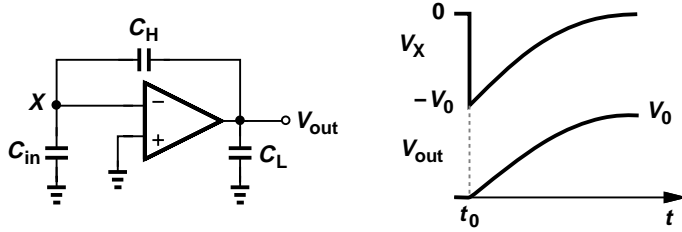


Figure 12.37. Time response of unity-gain sampler in amplification mode.

with $V_{out} \approx 0$ and eventually produce $V_{out} \approx V_0$. If C_{in} is relatively small, we can assume that the voltages across C_L and C_H do not change instantaneously, concluding that if $V_{out} \approx 0$ and $V_{CH} \approx V_0$, then $V_X = -V_0$ at the beginning of the amplification mode. In other words, the input difference sensed by the op amp initially jumps to a large value, possibly causing the op amp to slew. But, let us first assume the op amp can be modeled by a linear model and determine the output response.

To simplify the analysis, we represent the charge on C_H by an explicit series voltage source, V_S , that goes from zero to V_0 at $t = t_0$ while C_H carries no charge itself (Fig. 12.38). The objective is to obtain the transfer function $V_{out}(s)/V_S(s)$ and hence the step response. We have

$$V_{out}\left(\frac{1}{R_0} + C_{LS}\right) + G_m V_X = (V_0 + V_X - V_{out})C_H s. \quad (12.46)$$

Also, since the current through C_{in} equals $V_X C_{in} s$,

$$V_X \frac{C_{in}s}{C_H s} + V_X + V_S = V_{out}. \quad (12.47)$$

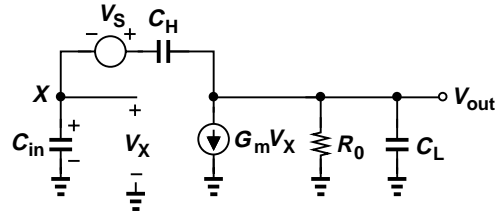


Figure 12.38. Equivalent circuit of unity-gain circuit in amplification mode.

Calculating V_X from (12.47) and substituting in (12.46), we arrive at the transfer function:

$$\frac{V_{out}}{V_S}(s) = R_0 \frac{(G_m + C_{in}s)C_H}{R_0(C_L C_{in} + C_{in} C_L + C_H C_L)s + G_m R_0 C_H + C_H + C_{in}}. \quad (12.48)$$

Note that for $s = 0$, (12.48) reduces to a form similar to (12.41). Since typically $G_m R_0 C_H \gg C_H, C_{in}$, we can simplify (12.48) as

$$\frac{V_{out}}{V_S}(s) = \frac{(G_m + C_{in}s)C_H}{(C_L C_{in} + C_{in} C_L + C_H C_L)s + G_m C_H}. \quad (12.49)$$

Thus, the response is characterized by a time constant equal to

$$\tau_{amp} = \frac{C_L C_{in} + C_{in} C_L + C_H C_L}{G_m C_H}, \quad (12.50)$$

which is independent of the op amp output resistance. This is because a higher R_0 leads to a greater loop gain, eventually yielding a constant closed-loop speed. If $C_{in} \ll C_L, C_H$, then (12.50) reduces to C_L/G_m , an expected result because with negligible C_{in} , the output resistance of the unity-gain buffer is equal to $1/G_m$.

We now study the slewing behavior of the circuit, considering a telescopic op amp as an example. Upon entering the amplification mode, the circuit may experience a large step at the inverting input (Fig. 12.37). As shown in Fig. 12.39, the tail current of the op amp's input differential pair is then steered to one side, charging the capacitance seen at the output. Since M_2 is off during slewing, C_{in} is negligible and the slew rate is approximately equal to I_{SS}/C_L . The slewing continues until V_X is sufficiently close to the gate voltage of M_1 , after which point the settling progresses with the time constant given in (12.50).

Our foregoing studies reveal that the input capacitance of the op amp degrades both the speed and the precision of the unity-gain sampler/buffer. For this reason, the bottom plate of C_H in Fig. 12.30 is usually driven by the input signal or the output of the op amp and the top plate is connected to node X (Fig. 12.40), minimizing the parasitic capacitance seen from node X to ground. This technique is called “bottom-plate sampling.”

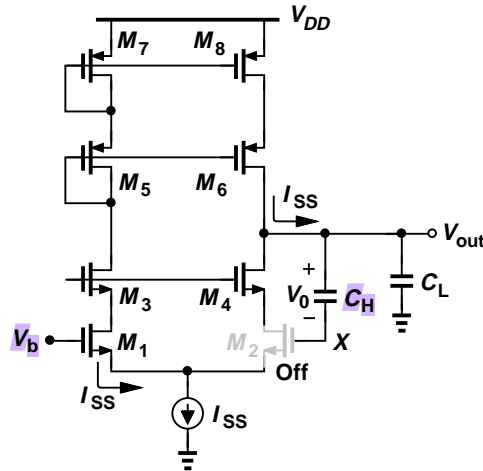


Figure 12.39. Unity-gain sampler during slewing.

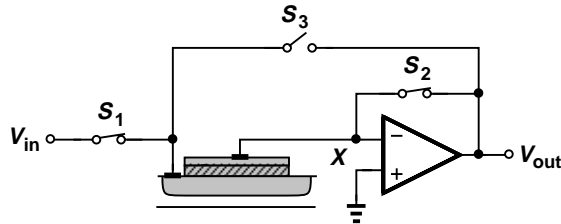


Figure 12.40. Connection of capacitor to the unity-gain sampler.

It is instructive to compare the performance of the sampling circuits shown in Figs. 12.29(b) and 12.30(a). In Fig. 12.29(b), the sampling time constant is smaller because it depends on only the on-resistance of the switch. More importantly, in Fig. 12.29(b), the amplification after the switch turns off is almost instantaneous whereas in Fig. 12.30, it requires a finite settling time. However, the critical advantage of the unity-gain sampler is the input-independent charge injection.

12.3.2 Noninverting Amplifier

In this section, we revisit the amplifier of Fig. 12.4, studying its speed and precision properties. Repeated in Fig. 12.41(a), the amplifier operates as follows. In the sampling mode, S_1 and S_3 are on and S_2 is off, creating a virtual ground at X and allowing the voltage across C_1 to track the input voltage [Fig. 12.41(b)]. At the end of the sampling mode, S_2 turns off first, injecting a constant charge, Δq_2 , onto node X . Subsequently, S_1 turns off and S_3 turns on [Fig. 12.41(c)]. Since V_P goes from V_{in0} to 0, the output voltage changes from 0 to approximately $V_{in0}(C_1/C_2)$, providing a voltage gain equal to C_1/C_2 . We call the circuit a “noninverting amplifier” because the final output has the same polarity as V_{in0} and the gain can be greater than unity.

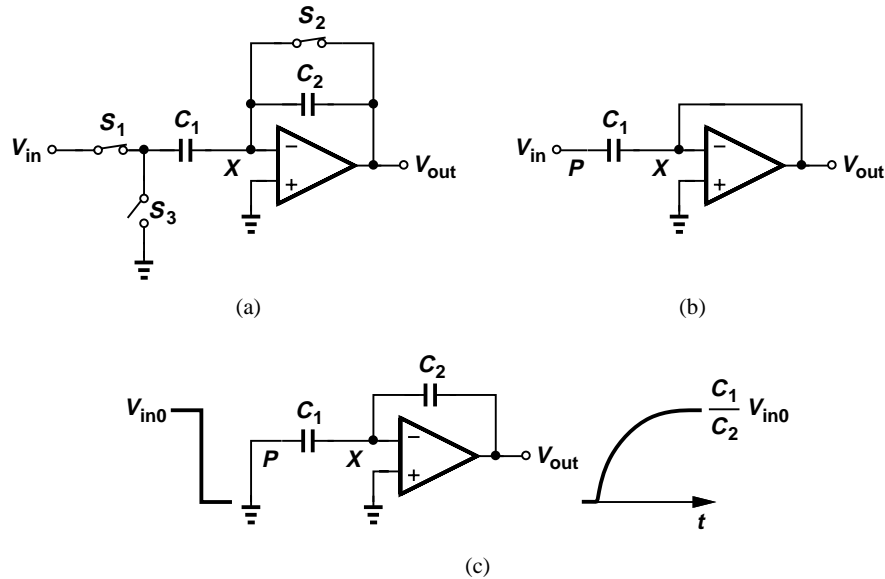


Figure 12.41. (a) Noninverting amplifier, (b) circuit of (a) in sampling mode, (c) transition of circuit to amplification mode.

As with the unity-gain circuit of Fig. 12.30(a), the noninverting amplifier avoids input-dependent charge injection by proper timing, namely, turning S_2 off before S_1 (Fig. 12.42). After S_2 is off, the total charge at node X remains constant, making the circuit insensitive to

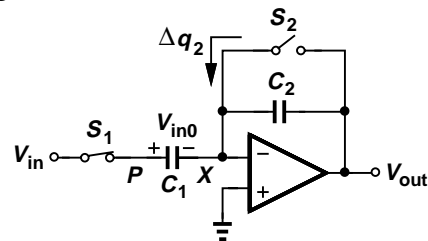


Figure 12.42. Transition of noninverting amplifier to amplification mode.

charge injection of S_1 or charge “absorption” of S_3 . Let us first study the effect of S_1 carefully. As illustrated in Fig. 12.43, the charge injected by S_1 , Δq_1 , changes the voltage at node P by approximately $\Delta V_P = \Delta q_1/C_1$, and hence the output voltage by $-\Delta q_1 C_1/C_2$. However, after S_3 turns on, V_P drops to zero. Thus, the overall change in V_P is equal to $0 - V_{in0} = -V_{in0}$, producing an overall change in the output equal to $-V_{in0}(-C_1/C_2) = V_{in0}C_1/C_2$.

The key point here is that V_P goes from a fixed voltage, V_0 , to another, 0, with an intermediate perturbation due to S_1 . Since the output voltage of interest is measured after node P is connected to ground, the charge injected by S_1 does not affect the final output. From another perspective, as shown in Fig. 12.44, the charge on the right plate of C_1 at the instant S_2 turns off is approximately

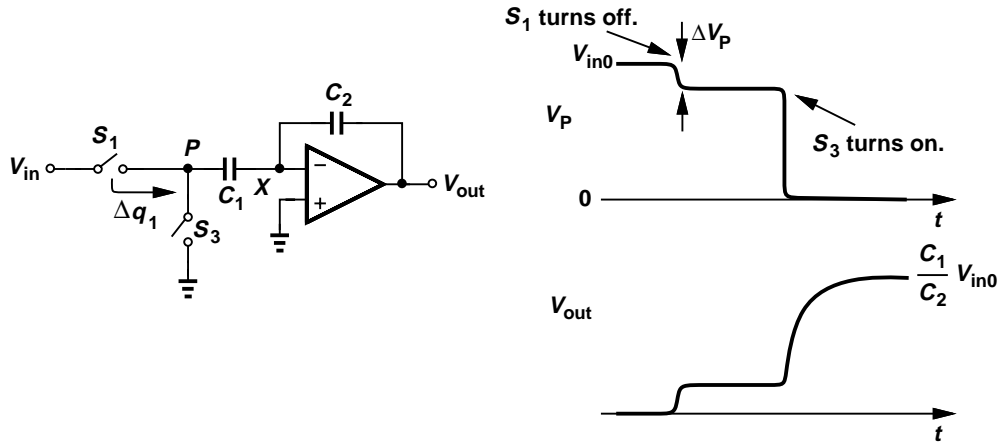
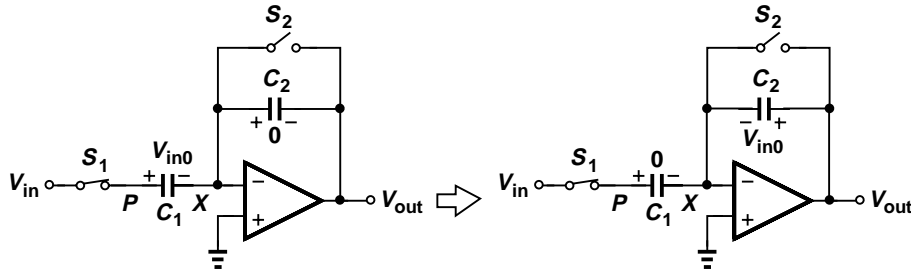
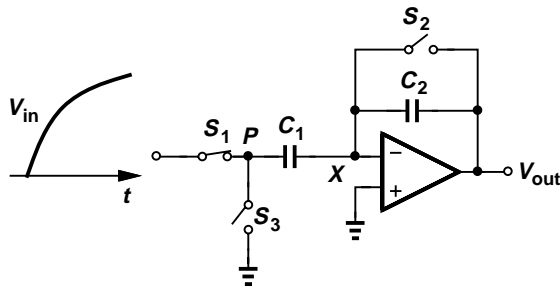
Figure 12.43. Effect of charge injected by S_1 .

Figure 12.44. Charge redistribution in noninverting amplifier.

equal to $-V_{in0}C_1$. Also, the total charge at node X must remain constant after S_2 turns off. Thus, when node P is connected to ground and the circuit settles, the voltage across C_1 and hence its charge are nearly zero, and the charge $-V_{in0}C_1$ must reside on the left plate of C_2 . In other words, the output voltage is approximately equal to V_{in0} regardless of the intermediate excursions at node P .

The foregoing discussion indicates that two other phenomena have no effect on the final output. First, from the time S_2 turns off until the time S_1 turns off, the input voltage may change significantly (Fig. 12.45) without introducing any error. In other words, the sampling instant is defined by the turn-off of S_2 . Second, when S_3 turns on, it requires some channel charge but since the final value of V_P is zero, this charge is unimportant. Neither of these effects introduces error because the total charge at node X is conserved and V_P is eventually set by a fixed (zero) potential. To emphasize that V_P is initially and finally determined by fixed voltages, we say node P is “driven” or node P switches from a low-impedance node to another low-impedance node. Here the term low-impedance distinguishes node P , at which charge is not conserved, from “floating” nodes such as X , where charge is conserved.

Figure 12.45. Effect of input change after S_2 turns off.

In summary, proper timing in Fig. 12.41(a) ensures that node X is perturbed by only the charge injection of S_2 , making the final value of V_{out} free from errors due to S_1 and S_3 . The constant offset due to S_2 can be suppressed by differential operation (Fig. 12.46).

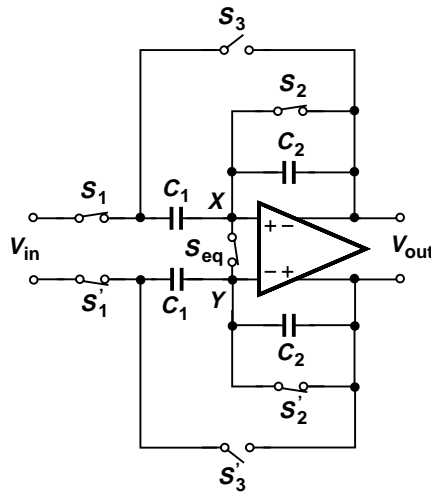


Figure 12.46. Differential realization of noninverting amplifier.

Example 12.4

In the differential circuit of Fig. 12.46, suppose the equalizing switch is not used and S_2 and S'_2 exhibit a threshold voltage mismatch of 10 mV. If $C_1 = 1 \text{ pF}$, $C_2 = 0.5 \text{ pF}$, $V_{TH} = 0.6 \text{ V}$, and for all switches $WLC_{ox} = 50 \text{ fF}$, calculate the dc offset measured at the output assuming all of the channel charge of S_2 and S'_2 is injected onto X and Y , respectively.

Solution. Simplifying the circuit as in Fig. 12.47, we have $V_{out} \approx \Delta q/C_2$, where $\Delta q = WLC_{ox}\Delta V_{TH}$. Note that C_1 does not appear in the result because X is a virtual ground, i.e., the voltage across C_1 changes only negligibly. Thus, the injected charge resides primarily on the left plate of C_2 , giving an output error voltage equal to $\Delta V_{out} = WLC_{ox}\Delta V_{TH}/C_2 = 1 \text{ mV}$.

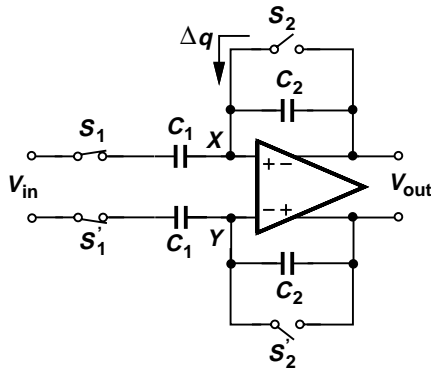


Figure 12.47.

Precision Considerations As mentioned above, the circuit of Fig. 12.41(a) provides a nominal voltage gain of C_1/C_2 . We now calculate the actual gain if the op amp exhibits a finite open-loop gain equal to A_{v1} . Depicted in Fig. 12.48 along with the input capacitance of the op amp, the

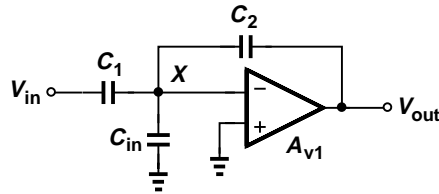


Figure 12.48. Equivalent circuit of noninverting amplifier during amplification.

circuit amplifies the input voltage change such that:

$$(V_{out} - V_X)C_2s = V_X C_{in}s + (V_X - V_{in})C_1s. \quad (12.51)$$

Since $V_{out} = -A_{v1}V_X$, we have

$$\frac{V_{out}}{V_{in}} = \frac{-C_1}{C_2 + \frac{C_2 + C_1 + C_{in}}{A_{v1}}}. \quad (12.52)$$

For large A_{v1} ,

$$\frac{V_{out}}{V_{in}} \approx -\frac{C_1}{C_2} \left(1 - \frac{C_2 + C_1 + C_{in}}{C_2} \cdot \frac{1}{A_{v1}}\right), \quad (12.53)$$

implying that the amplifier suffers from a gain error of $(C_2 + C_1 + C_{in})/(C_2 A_{v1})$. Note that the gain error increases with the nominal gain C_1/C_2 .

Comparing (12.42) with (12.53), we note that with $C_H = C_2$ and for a nominal gain of unity, the noninverting amplifier exhibits greater gain error than does the unity-gain sampler. This is because

the feedback factor equals $C_2/(C_1 + C_{in} + C_2)$ in the former and $C_H/(C_H + C_{in})$ in the latter. For example, if C_{in} is negligible, the unity-gain buffer's gain error is half that of the noninverting amplifier.

Speed Considerations The smaller feedback factor in Fig. 12.48 suggests that the time response of the amplifier may be slower than that of the unity-gain sampler. This is indeed true. Consider the equivalent circuit shown in Fig. 12.49(a). Since the only difference between this circuit and that

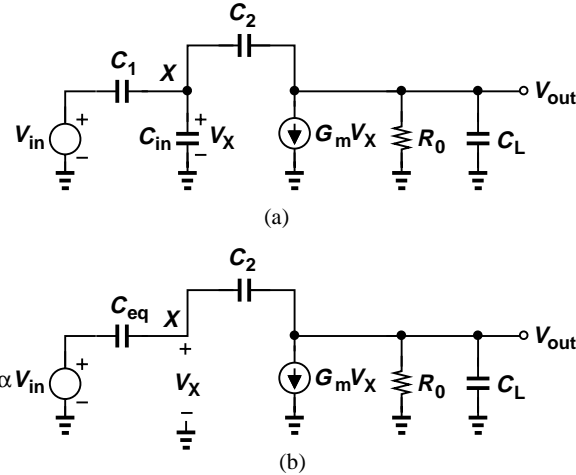


Figure 12.49. (a) Equivalent circuit of noninverting amplifier in amplification mode, (b) circuit of (a) with V_{in} , C_1 , and C_{in} replaced by a Thevenin equivalent.

in Fig. 12.38 is the capacitor C_1 , which is connected from node X to an ideal voltage source, we expect that (12.50) gives the time constant of this amplifier as well if C_{in} is replaced by $C_{in} + C_1$. But for a more rigorous analysis, we substitute V_{in} , C_1 , and C_{in} in Fig. 12.49(a) by a Thevenin equivalent as in Fig. 12.49(b), where $\alpha = C_1 / (C_1 + C_{in})$, and $C_{eq} = C_1 + C_{in}$, and note that

$$V_X = (\alpha V_{in} - V_{out}) \frac{C_{eq}}{C_{eq} + C_2} + V_{out}. \quad (12.54)$$

Thus,

$$[(\alpha V_{in} - V_{out}) \frac{C_{eq}}{C_{eq} + C_2} + V_{out}] G_m + V_{out} \left(\frac{1}{R_0} + C_L s \right) = (\alpha V_{in} - V_{out}) \frac{C_{eq} C_2}{C_{eq} + C_2} s, \quad (12.55)$$

and hence

$$\frac{V_{out}(s)}{V_{in}} = \frac{-C_{eq} \frac{C_1}{C_1 + C_{in}} (G_m - C_2 s) R_0}{C_2 G_m R_0 + C_{eq} + C_2 + R_0 [C_L (C_{eq} + C_2) + C_{eq} C_2] s}. \quad (12.56)$$

Note that for $s = 0$, (12.56) reduces to (12.52). For a large $G_m R_0$, we can simplify (12.56) to

$$\frac{V_{out}}{V_{in}}(s) \approx \frac{-C_{eq} \frac{C_1}{C_1 + C_{in}} (G_m - C_2 s) R_0}{R_0(C_L C_{eq} + C_L C_2 + C_{eq} C_2)s + G_m R_0 C_2}, \quad (12.57)$$

obtaining a time constant of

$$\tau_{amp} = \frac{C_L C_{eq} + C_L C_2 + C_{eq} C_2}{G_m C_2}, \quad (12.58)$$

which is the same as the time constant of Fig. 12.37 if C_{in} is replaced by $C_{in} + C_1$. Note the direct dependence of τ_{amp} upon the nominal gain, C_1/C_2 .

It is instructive to examine the amplifier's time constant for the special case $C_L = 0$. Equation (12.58) yields $\tau_{amp} = (C_1 + C_{in})/G_m$, a value *independent* of the feedback capacitor. This is because, while a larger C_2 introduces **heavier loading at the output**, it also provides a **greater feedback factor**.

12.3.3 Precision Multiply-by-Two Circuit

The circuit of Fig. 12.41(a) can operate with a relatively high closed-loop gain, but it suffers from speed and precision degradation due to the **low feedback factor**. In this section, we study a topology that provides a nominal gain of two while achieving a higher speed and lower gain error [5]. Shown in Fig. 12.50(a), the amplifier incorporates two equal capacitors, $C_1 = C_2 = C$. In the sampling mode, the circuit is configured as in Fig. 12.50(b), establishing a virtual ground at X and allowing the voltage across C_1 and C_2 to track V_{in} . In the transition to the amplification mode, S_3 turns off first, C_1 is placed around the op amp, and the left plate of C_2 is switched to ground [Fig. 12.50(c)]. Since at the moment S_3 turns off, the total charge on C_1 and C_2 equals $2V_{in0}C$ (if the charge injected by S_3 is neglected), and since the voltage across C_2 approaches zero in the amplification mode, the final voltage across C_1 and hence the output voltage are approximately equal to $2V_{in0}$. This can also be seen from the slow motion illustration of Fig. 12.51.

The reader can show that the charge injected by S_1 and S_2 and absorbed by S_4 and S_5 is unimportant and that injected by S_3 introduces a constant offset. The offset can be suppressed by differential operation.

The speed and precision of the multiply-by-two circuit are expressed by (12.58) and (12.53), respectively, but the advantage of the circuit is the higher feedback factor for a given closed-loop gain. Note, however, that the input capacitance of the multiply-by-two circuit in the sampling mode is higher.

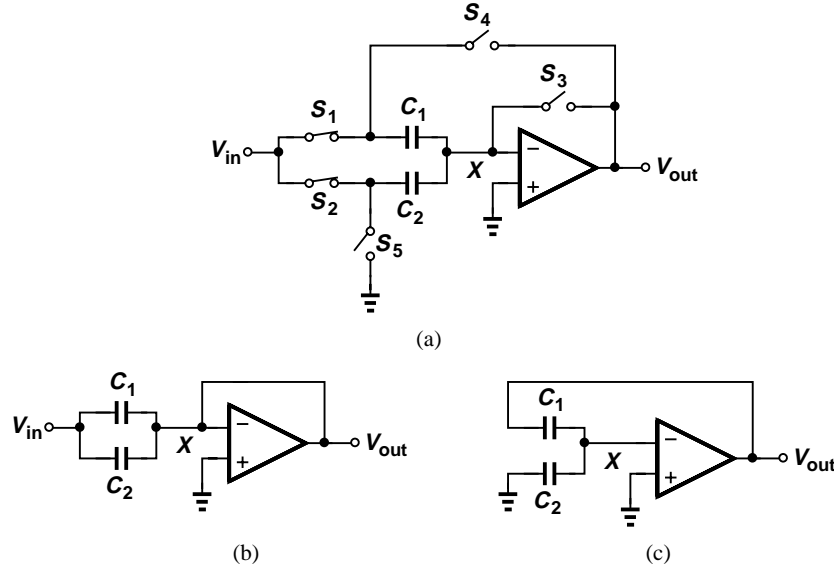


Figure 12.50. (a) Multiply-by-two circuit, (a) circuit of (a) in sampling mode, (b) circuit of (a) in amplification mode.

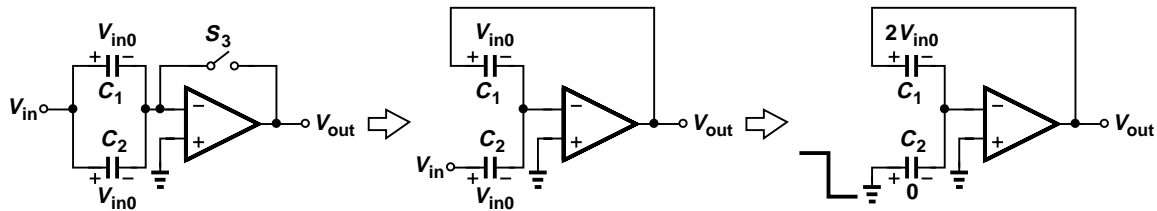


Figure 12.51. Transition of multiply-by-two-circuit to amplification mode in slow motion.

12.4 Switched-Capacitor Integrator

Integrators are used in many analog systems. Examples include filters and oversampled analog-to-digital converters. Fig. 12.52 depicts a continuous-time integrator, whose output can be expressed

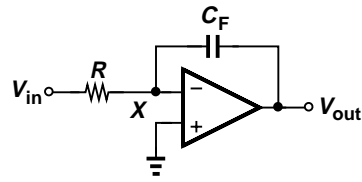


Figure 12.52. Continuous-time integrator.

as

$$V_{out} = -\frac{1}{RC_F} \int V_{in} dt, \quad (12.59)$$

if the op amp gain is very large. For sampled-data systems, we must devise a discrete-time counterpart of this circuit.

Before studying SC integrators, let us first point out an interesting property. Consider a resistor connected between two nodes [Fig. 12.53(a)], carrying a current equal to $(V_A - V_B)/R$. The role

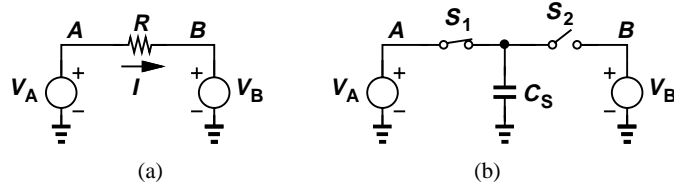


Figure 12.53. (a) Continuous-time and (b) discrete-time resistors.

of the resistor is to take a certain amount of charge from node A every second and move it to node B . Can we perform the same function by a capacitor? Suppose in the circuit of Fig. 12.53(b), capacitor C_S is alternately connected to nodes A and B at a clock rate f_{CK} . The *average* current flowing from A to B is then equal to the charge moved in one clock period:

$$\overline{I_{AB}} = \frac{C_S(V_A - V_B)}{f_{CK}^{-1}} \quad (12.60)$$

$$= C_S f_{CK} (V_A - V_B). \quad (12.61)$$

We can therefore view the circuit as a “resistor” equal to $(C_S f_{CK})^{-1}$. Recognized by James Clark Maxwell, this property formed the foundation for many modern switched-capacitor circuits.

Let us now replace resistor R in Fig. 12.52 by its discrete-time equivalent, arriving at the integrator of Fig. 12.54(a). We note that in every clock cycle, C_1 absorbs a charge equal to $C_1 V_{in}$

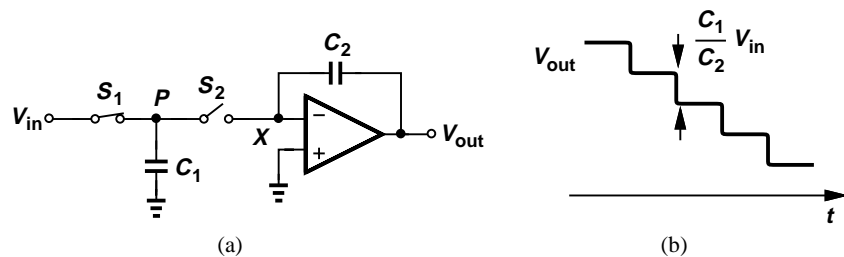


Figure 12.54. (a) Discrete-time integrator, (b) response of circuit to a constant input voltage.

when S_1 is on and deposits the charge on C_2 when S_2 is on (node X is a virtual ground). For example, if V_{in} is constant, the output changes by $V_{in} C_1 / C_2$ every clock cycle [Fig. 12.54(b)]. Approximating the staircase waveform by a ramp, we note that the circuit behaves as an integrator.

The final value of V_{out} in Fig. 12.54(a) after every clock cycle can be written as

$$V_{out}(kT_{CK}) = V_{out}[(k-1)T_{CK}] - V_{in}[(k-1)T_{CK}] \cdot \frac{C_1}{C_2}, \quad (12.62)$$

where the gain of the op amp is assumed large. Note that the small-signal settling time constant as charge is transferred from C_1 to C_2 is given by (12.50).

The integrator of Fig. 12.54(a) suffers from two important drawbacks. First, the input-dependent charge injection of S_1 introduces nonlinearity in the charge stored on C_1 and hence the output voltage. Second, the nonlinear capacitance at node P resulting from the source/drain junctions of S_1 and S_2 leads to a nonlinear charge-to-voltage conversion when C_1 is switched to X . This can be understood with the aid of Fig. 12.55, where the charge stored on the total junction capacitance, C_j , is *not* equal to $V_{in0}C_j$, but rather equal to

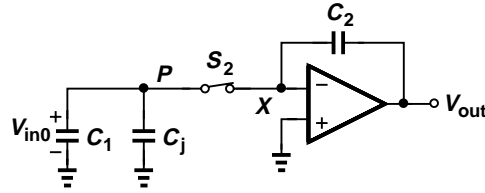


Figure 12.55. Effect of junction capacitance nonlinearity in SC integrator.

$$q_{cj} = \int_0^{V_{in0}} C_j dV. \quad (12.63)$$

Since C_j is a function of voltage, q_{cj} exhibits a nonlinear dependence on V_{in0} , thereby creating a nonlinear component at the output after the charge is transferred to the integration capacitor.

An integrator topology that resolves both of the foregoing issues is shown in Fig. 12.56(a). We study the circuit's operation in the sampling and integration modes. As shown in Fig. 12.56(b), in the sampling mode S_1 and S_3 are on and S_2 and S_4 are off, allowing the voltage across C_1 to track V_{in} while the op amp and C_2 hold the previous value. In the transition to the integration mode, S_3 turns off first, injecting a constant charge onto C_1 , S_1 turns off next, and subsequently S_2 and S_4 turn on [Fig. 12.56(c)]. The charge stored on C_1 is therefore transferred to C_2 through the virtual ground node.

Since S_3 turns off first, it introduces only a constant offset, which can be suppressed by differential operation. Moreover, because the left plate of C_1 is “driven” (Section 12.3.2), the charge injection or absorption of S_1 and S_2 contributes no error. Also, since node X is a virtual ground, the charge injected or absorbed by S_4 is constant and independent of V_{in} .

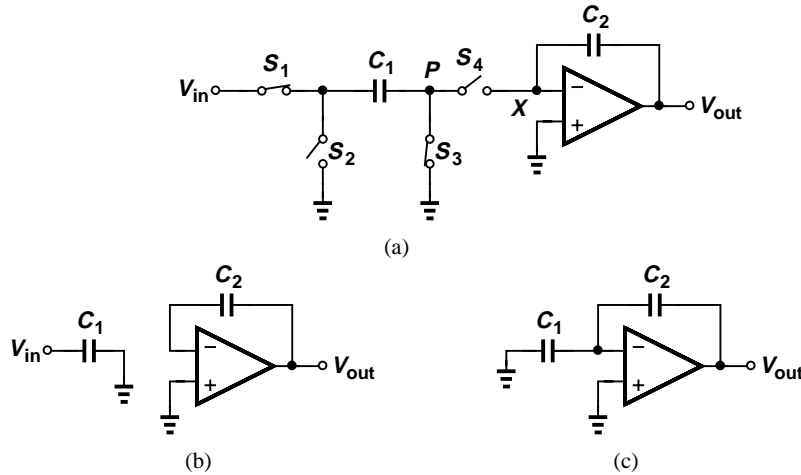


Figure 12.56. (a) Parasitic-insensitive integrator, (b) circuit of (a) in sampling mode, (c) circuit of (a) in integration mode.

How about the nonlinear junction capacitance of S_3 and S_4 ? We observe that the voltage across this capacitance goes from near zero in the sampling mode to virtual ground in the integration mode. Since the voltage across the nonlinear capacitance changes by a very small amount, the resulting nonlinearity is negligible.

12.5 Switched-Capacitor Common-Mode Feedback

Our study of common-mode feedback in Chapter 9 suggested that sensing the output CM level by means of resistors lowers the differential voltage gain of the circuit considerably. We also observed that sensing techniques using MOSFETs that operate as source followers or variable resistors suffer from a limited linear range. Switched-capacitor CMFB networks provide an alternative that avoids both of these difficulties (but the circuit must be refreshed periodically.)

In switched-capacitor common-mode feedback, the outputs are sensed by capacitors rather than resistors. Figure 12.57 depicts a simple example, where equal capacitors C_1 and C_2 reproduce at node X the average of the changes in each output voltage. Thus, if V_{out1} and V_{out2} experience a, say, positive CM change, then V_X and hence I_{D5} increase, pulling V_{out1} and V_{out2} down. The output CM level is then equal to V_{GS2} plus the voltage across C_1 and C_2 .

How is the voltage across C_1 and C_2 defined? This is typically carried out when the amplifier is in the sampling (or reset) mode and can be accomplished as shown in Fig. 12.58. Here, during CM level definition, the amplifier differential input is zero and switch S_1 is on. Transistors M_6 and M_7 operate as a linear sense circuit because their gate voltages are nominally equal. Thus, the circuit settles such that the output CM level is equal to $V_{GS6,7} + V_{GS5}$. At the end of this mode, S_1

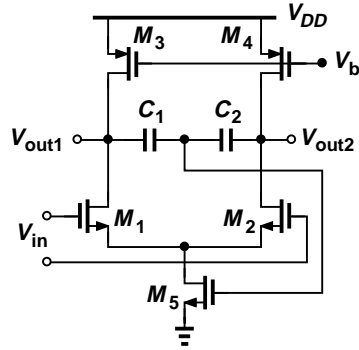
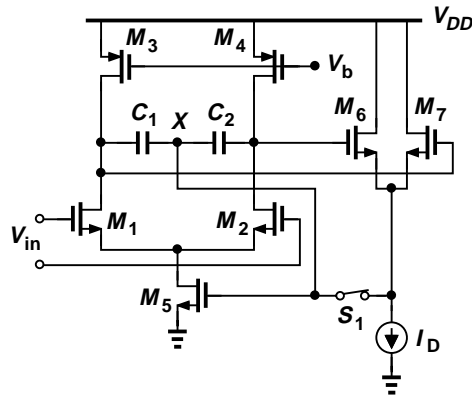


Figure 12.57. Simple SC common-mode feedback.

Figure 12.58. Definition of the voltage across C_1 and C_2 .

turns off, leaving a voltage equal to $V_{GS5,6}$ across C_1 and C_2 . In the amplification mode, M_6 and M_7 may experience a large nonlinearity but they do not impact the performance of the main circuit because S_1 is off.

In applications where the output CM level must be defined more accurately than in the above example, the topology shown in Fig. 12.59 may be used. Here, in the reset mode, one plate of C_1

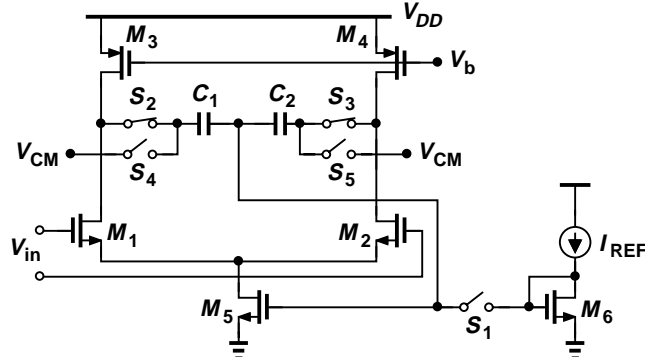


Figure 12.59. Alternative topology for definition of output CM level.

and C_2 is switched to V_{CM} while the other is connected to the gate of M_6 . Each capacitor therefore sustains a voltage equal to $V_{CM} - V_{GS6}$. In the amplification mode, S_2 and S_3 are on and the other switches are off, yielding an output CM level equal to $V_{CM} - V_{GS6} + V_{GS5}$. Proper definition of I_{D3} and I_{D4} with respect to I_{REF} can guarantee that $V_{GS5} = V_{GS6}$ and hence the output CM level is equal to V_{CM} .

With large output swings, the speed of the CMFB loop may in fact influence the settling of the differential output [6]. For this reason, part of the tail current of the differential pairs in Figs. 12.58 and 12.59 can be provided by a *constant* current source so that M_5 makes only small adjustments to the circuit.

Problems

Unless otherwise stated, in the following problems, use the device data shown in Table 2.1 and assume $V_{DD} = 3$ V where necessary. Also, assume all transistors are in saturation.

12.1 The circuit of Fig. 12.2(a) is designed with $C_1 = 2$ pF and $C_2 = 0.5$ pF.

- (a) Assuming $R_F = \infty$ but the op amp has an output resistance R_{out} , derive the transfer function $V_{out}(s)/V_{in}(s)$.
- (b) If the op amp is ideal, determine the minimum value of R_F that guarantees a gain error of 1% for an input frequency of 1 MHz.

12.2 Suppose in Fig. 12.5(a), the op amp is characterized by a transconductance G_m and an output resistance R_{out} .

- (a) Determine the transfer function V_{out}/V_{in} in this mode.
- (b) Plot the waveform at node B if V_{in} is a 100-MHz sinusoid with a peak amplitude of 1 V, $C_1 = 1$ pF, $G_m = 1/(100 \Omega)$, and $R_{out} = 20$ k Ω .

12.3 In Fig. 12.5(b), node A is in fact connected to ground through a switch (Fig. 12.4). If the switch introduces a series resistance R_{on} and the op amp is ideal, calculate the time constant of the circuit in this mode. What is the total energy dissipated in the switch as the circuit enters the amplification mode and V_{out} settles to its final value?

12.4 The circuit of Fig. 12.9(a) is designed with $(W/L)_1 = 20/0.5$ and $C_H = 1$ pF.

- (a) Using Eqs. (12.7) and (12.14), calculate the time required for V_{out} to drop to +1 mV.
- (b) Approximating M_1 by a linear resistor equal to $[\mu_n C_{ox} (W/L)_1 (V_{DD} - V_{TH})]^{-1}$, calculate the time required for V_{out} to drop to +1 mV and compare the result with that obtained in part (a).

12.5 The circuit of Fig. 12.11 cannot be characterized by a single time constant because the resistance charging C_H (equal to $1/g_{m1}$ if $\gamma = 0$) varies with the output level. Assume $(W/L)_1 = 20/0.5$ and $C_H = 1 \text{ pF}$.

(a) Using Eq. (12.19), calculate the time required for V_{out} to reach 2.1 V.

(b) Sketch the transconductance of M_1 versus time.

12.6 In the circuit of Fig. 12.8(b), $(W/L)_1 = 20/0.5$ and $C_H = 1 \text{ pF}$. Assume $\lambda = \gamma = 0$ and $V_{in} = V_0 \sin \omega_{in} t + V_m$, where $\omega_{in} = 2\pi \times (100 \text{ MHz})$.

(a) Calculate R_{on1} and the phase shift from the input to the output if $V_0 = V_m = 10 \text{ mV}$.

(b) Repeat part (a) if $V_0 = 10 \text{ mV}$ but $V_m = 1 \text{ V}$. The variation of the phase shift translates to distortion.

12.7 Describe an efficient SPICE simulation that yields the plot of $R_{on,eq}$ for the circuit of Fig. 12.16.

12.8 The sampling network of Fig. 12.16 is designed with $(W/L)_1 = 20/0.5$ and $(W/L)_2 = 60/0.5$. If $V_{in} = 0$ and the initial value of V_{out} is +3 V, estimate the time required for V_{out} to drop to +1 mV.

12.9 In the circuit of Fig. 12.19, $(W/L)_1 = 20/0.5$ and $C_H = 1 \text{ pF}$. Calculate the maximum error at the output due to charge injection. Compare this error with that resulting from clock feedthrough.

12.10 The circuit of Fig. 12.60 samples the input on C_1 when CK is high and connects C_1 and C_2

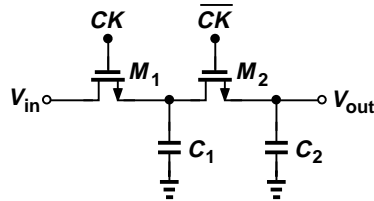


Figure 12.60.

when CK is low. Assume $(W/L)_1 = (W/L)_2$ and $C_1 = C_2$.

(a) If the initial voltages across C_1 and C_2 are zero and $V_{in} = 2 \text{ V}$, plot V_{out} versus time for many clock cycles. Neglect charge injection and clock feedthrough.

(b) What is the maximum error in V_{out} due to charge injection and clock feedthrough of M_1 and M_2 ? Assume the channel charge of M_2 splits equally between C_1 and C_2 .

(c) Determine the kT/C noise at the output after M_2 turns off.

12.11 For $V_{in} = V_0 \sin \omega_0 t + V_0$, where $V_0 = 0.5$ V and $\omega_0 = 2\pi \times (10 \text{ MHz})$, plot the output waveforms of the circuits shown in Fig. 12.29(b) and 12.30(a). Assume a clock frequency of 50 MHz.

12.12 In Fig. 12.45, S_1 turns off Δt seconds after S_2 and S_3 turns on Δt seconds after S_1 turns off. Plot the output waveform, taking into account the charge injection and clock feedthrough of S_1-S_3 .

12.13 The circuit of Fig. 12.48 is designed with $C_1 = 2 \text{ pF}$, $C_{in} = 0.2 \text{ pF}$ and $A_v = 1000$. What is the maximum nominal gain, C_1/C_2 , that the circuit can provide with a gain error of 1%?

12.14 In Problem 12.13, what is the maximum nominal gain if $G_m = 1/(100 \Omega)$ and the circuit must achieve a time constant of 2 ns in the amplification mode?

12.15 The integrator of Fig. 12.54 is designed with $C_1 = C_2 = 1 \text{ pF}$ and a clock frequency of 100 MHz. Neglecting charge injection and clock feedthrough, sketch the output if the input is a 10-MHz sinusoid with a peak amplitude of 0.5 V. Approximating C_1 , S_1 , and S_2 by a resistor, estimate the output amplitude.

12.16 Consider the switched-capacitor amplifier depicted in Fig. 12.61, where the common-mode

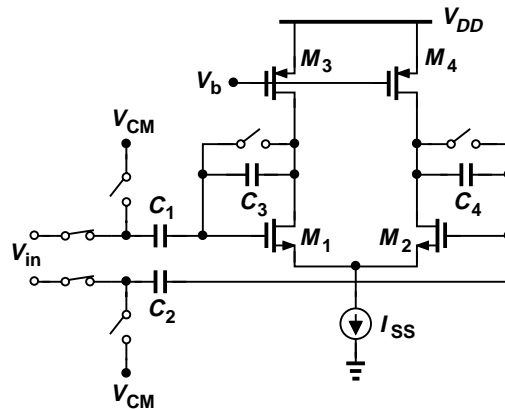


Figure 12.61.

feedback is not shown. Assume $(W/L)_{1-4} = 50/0.5$, $I_{SS} = 1 \text{ mA}$, $C_1 = C_2 = 2 \text{ pF}$, $C_3 = C_4 = 0.5 \text{ pF}$, and the output CM level is 1.5 V. Neglect the transistor capacitances.

(a) What is the maximum allowable output voltage swing in the amplification mode?

- (b) Determine the gain error of the amplifier.
 (c) What is the small-signal time constant in the amplification mode?

12.17 Repeat Problem 12.16 if the gate-source capacitance of M_1 and M_2 is not neglected.

12.18 A differential circuit incorporating a well-designed common-mode feedback network exhibits the open-loop input-output characteristic shown in Fig. 12.62(a). In some circuits, however, the characteristic appears as in Fig. 12.62(b). Explain how this effect occurs.

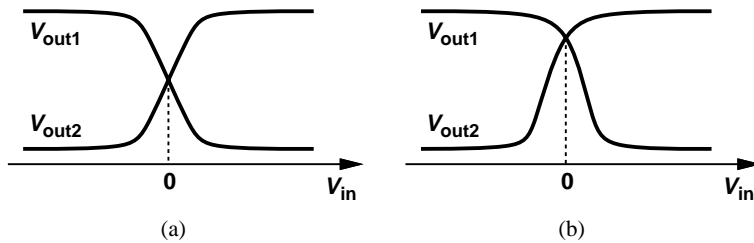


Figure 12.62.

12.19 In the common-mode feedback network of Fig. 12.58, assume $W/L = 50/0.5$ for all transistors, $I_{D5} = 1 \text{ mA}$, and $I_{D6,7} = 50 \mu\text{A}$. Determine the allowable range of the input common-mode level.

12.20 Repeat Problem 12.19 if $(W/L)_{5,6} = 10/0.5$.

12.21 Suppose in the common-mode feedback network of Fig. 12.58, S_1 injects a charge of Δq onto the gate of M_5 . How much do the gate voltage of M_5 and the output common-mode level change due to this error?

12.22 In the circuit of Fig. 12.63, each op amp is represented by a Norton equivalent and characterized by G_m and R_{out} . The output currents of two op amps are summed at node Y [7]. (The circuit is shown in the amplification mode.) Note that the main amplifier and the auxiliary amplifier are identical and the error amplifier senses the voltage variation at node X and injects a proportional current into node Y . Assume $G_m R_{out} \gg 1$.

- (a) Calculate the gain error of the circuit.
 (b) Repeat part (a) if the auxiliary and error amplifiers are eliminated and compare the results.

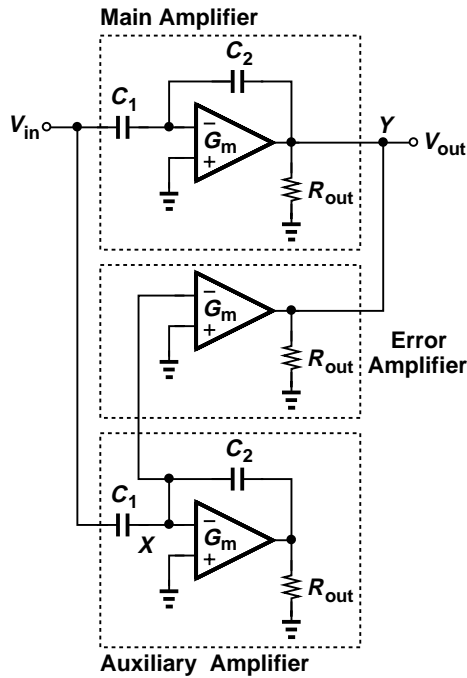


Figure 12.63.

References

- [1] G. Wegmann, E. A. Vittoz, and F. Rahali, "Charge Injection in Analog MOS Switches," *IEEE J. Solid-State Circuits*, vol. SC-22, pp. 1091-1097, Dec. 1987.
- [2] B. J. Sheu and C. Hu, "Switch-Induced Error Voltage on a Switched Capacitor," *IEEE J. Solid-State Circuits*, vol. SC-19, pp. 519-525, April 1984.
- [3] R. Gregorian and G. C. Temes, *Analog MOS Integrated Circuits for Signal Processing*, John Wiley and Sons, New York, 1986.
- [4] J. H. Fischer, "Noise Sources and Calculation Techniques for Switched Capacitor Filters," *IEEE J. Solid-State Circuits*, vol. 17, pp. 742-752, Aug. 1982.
- [5] B. S. Song, M. F. Tompsett, and K. R. Lakshmikumar, "A 12-Bit 1-Msample/s Capacitor-Averaging Pipelined A/D Converter," *IEEE J. Solid-State Circuits*, vol. SC-23, pp. 1324-1333, Dec. 1988.
- [6] B. Razavi, *Principles of Data Conversion System Design*, IEEE Press, New York, 1995.
- [7] P. C. Yu and H.-S. Lee, "A High-Swing 2-V CMOS Op Amp with Replica-Amp Gain Enhancement," *IEEE J. Solid-State Circuits*, vol. 28, pp. 1265-1272, Dec. 1993.